Publised in Sustainable Energy, Grids and Neworks with doi: 10.1016/j.segan.2023.101088

An Interval-based Bi-level Day-ahead Scheduling Strategy for Active Distribution Networks in the Presence of Energy Communities

Marcos Tostado-Véliz[1], Yingqi Liang[2], Ahmad Rezaee Jordehi[3], Seyed Amir Mansouri[4], Francisco Jurado[1,*]

1. Department of Electrical Engineering, University of Jaén, 23700 Linares, Spain (e-mail: mtostado@ujaen.es (M.T.-V.), fjurado@ujaen.es (F.J.)).
2. Department of Electrical and Computer Engineering, National University of Singapore, Singapore 117576, Singapore (e-mail: yingqi.liang@u.nus.edu).
3. Department of Electrical Engineering, Rasht Branch, Islamic Azad University, Rasht 43, Iran (e-mail: ahmadrezaeejordehi@gmail.com).
4. Electrical Power and Control Systems Research Group, Northumbria University, UK (e-mail: amir.mansouri24@gmail.com).

* Correspondence: fjurado@ujaen.es.

Abstract. The decarbonization of the electricity sector calls for new operational schemes and businesses. In this context, traditional consumers have evolved towards prosumers, enabling the active participation of domestic installations in the system operation. A set of prosumers can be organized into energy communities to unlock different economic and energy benefits. This paper develops a bi-level scheduling strategy for robust optimal operation of active distribution networks in the presence of energy communities. The new proposal deals with energy management in communities at the lower level while managing distributed assets at the upper level. The uncertainties in demand, renewable generation, and energy prices are modeled using interval notation, which allows to adopt pessimistic or optimistic strategies. In addition, a novel Stackelberg-bisection sub-module is advocated to determine the distribution system operator profit, which considers collective welfare. The developed Mixed-Integer-Linear programming framework is tested in the IEEE 33-bus network incorporating energy communities, passive consumers, and distributed assets. The results obtained serve to validate the new methodology as well as analyse different results. For example, it is observed that the adopted strategy directly impacts the monetary balance, thus varying the incomes by up to 28 % depending on the robustness level. The proposed Stackelberg-based sub-module is also analysed, indicating that the expected profit may vary by up to 3 % depending on the strategy adopted and the level of robustness assumed.

Keywords. Distributed generation; Energy community; Interval optimization; Stackelberg game.

Nomenclature

Acronyms	
BES	Battery energy storage
CA	Controllable appliance
DG	Distributed generator
DN	Distribution network
DR	Demand response
DSO	Distribution system operator
EC	Energy community
EV	Electric vehicle
HVAC	Heating-ventilation-air conditioner
KKT	Karush-Kuhn-Tucker
MILP	Mixed integer linear programming
MINLP	Mixed integer nonlinear programming
P2P	Peer-to-peer
PV	Photovoltaic
SOC	State-of-charge

Sets	
$\boldsymbol{\Theta}$	Allowable time windows
$\boldsymbol{\mathcal{B}}$	Buses
$\boldsymbol{\mathcal{S}}$	Distributed energy storage systems
$\boldsymbol{\mathcal{G}}$	Distributed generators
$\boldsymbol{\mathcal{EC}}$	Energy communities
$\boldsymbol{\mathcal{A}}^{I/NI}$	Interruptible/non-interruptible controllable appliances
$\boldsymbol{\mathcal{C}}$	Passive consumers
$\boldsymbol{\mathcal{P}}$	Prosumers
$\boldsymbol{\mathcal{T}}$	Time
$\boldsymbol{\Omega}$	Uncertainties

Superscripts	
$BES, ch/dch$	Battery energy storage in charging/discharging mode
DN	Distribution network
$EV, ch/dch$	Electric vehicle in charging/discharging mode
EC	Energy community
$hot/cool$	Heating/cooling mode
$HVAC$	Heater-ventilation-air conditioner system
$buy/sell$	Imported/exported energy
$Air, in/out$	Indoor/outdoor air
$\underline{(*)}/\overline{(*)}$	Minimum/maximum value
NC	Non-controllable demand
$P2P$	Peer-to-peer energy exchanging
PV	Photovoltaic unit
sp/db	Set-point/dead-band
UG	Utility grid

Constants and parameters	
r	Branch resistance [ohm]
COP	Coefficient of performance [pu]
λ	DSO profit [pu]
DC	Duty cycle [h]
η	Efficiency [pu]

π	Energy price [$/kWh]
e2P	Energy-to-power ratio [h]
C	Heat capacity [kJ/(kg·°C)]
M	Mass [kg]
T	Temperature [°C]
R^{Build}	Thermal resistance of the building [J/°C]
Δt	Time step [h]
$\mathbb{E}[*]$	Expected value
$tol_{\sim}$	It refers to tolerances in iterative algorithms [-]
ξ	Uncertain level [pu]

Decision variables

on/off	Activation/deactivation status [binary]
p	Active power injection [kW]
P	Active power flow [kW]
u	Commitment status [binary]
ε	Energy [kWh]
V	Nodal voltage [V]

1 - Introduction

1.1 - Context & motivation

The effects of climate change and geopolitical conflicts have increased the necessity of reducing energy consumption worldwide [1]. Consequently, numerous European countries launched energy-saving programs in 2022 [2, 3] to reduce electricity consumption and thus minimize the dependency on natural gas exported from other countries. Under this paradigm, distributed generators (DGs), primarily based on renewable sources, will play a vital role in providing a clean and safe energy supply [4]. In contrast to conventional large-scale generators, DGs are located near to consumers, facilitating local energy supplying. However, this emerging framework poses formidable challenges, notably complicating the operation of distribution networks (DNs) that have evolved from passive to active systems [5].

This power system structure calls up for new agents and businesses like distribution system operators (DSOs), who are responsible for operating and maintaining distributed assets, including DGs [6]. This agent is keen to encourage the active participation of final users through demand response (DR) initiatives. In this way, final users can partake by leveraging their own resources, such as photovoltaic (PV) rooftop panels or small-scale battery energy storage (BES) banks [7]. To facilitate and promote the active participation of domestic users, they can be gathered into energy communities (ECs). This new concept enables the centralized operation of a group of consumers who provide local generation/storage to pursue collective welfare [8]. In this context, the interaction among ECs and DSO is clear and direct as the formers are directly connected to DNs. Hence, it is necessary to develop novel computational tools suitable for optimal coordination of DSOs and ECs, in order to operate both systems in an optimal way taking into account the multiple uncertainties brought by renewable generation, dynamic energy prices and electricity demand [9].

1.2 - Literature review

Although ECs are gaining importance owing to recent legislative development [10], they became to be studied seriously at early 2010’s [11]. Some very preliminary works focused on studying the viability of different technologies in such frameworks [12]. Nevertheless, the importance of energy management tools in ECs was firstly identified in [13], being nowadays accepted as an ideal practise to optimally exploit the available resources. Since then, the number of works dealing with energy management in ECs increased. Nowadays, the feasibility of ECs is totally accepted from a technical, economic and legislative point of view [14], as demonstrated various real-life projects worldwide [15].

Uncertainties modelling in active DNs is a hot topic profusely studied during years (see review in [16]). The strong uncertain behavior of these systems is caused by intermittent character of renewable DGs, but also inferred by dynamic prices or random consumption patterns. However, literature about uncertainty modelling in ECs is still limited, and such an EC system adds additional uncertain sources from numerous small-scale renewable generators and dispersed residential consumptions. Existing works frequently assume deterministic conditions, while only very few works consider simple stochastic approaches or other uncertain models that do not account for the interaction with the grid. In this regard, only a few works account for the coordination among DSO and prosumers, but only from a deterministic point of view.

In [17], a deterministic and optimal design/operation model for multi-energy communities encompassing storage devices was developed. The resulting Mixed-Integer Nonlinear Programming (MINLP) problem is decomposed into tractable subsystems to reduce the computational complexity of calculations. An optimal day-ahead scheduling tool for cooperative ECs was developed in [18]. The resulting formulation is based on the alternating direction of multipliers and accounts for peer-to-peer (P2P) energy transactions among prosumers. Jo et al. [19] focused on the role of customer-based storage devices in ECs. For this, a Mixed Integer Linear Programming (MILP) framework was proposed to optimally coordinate the community's storage assets, including the internal market mechanism for sharing storage capacity. Feng, et al. [20], presented a game-based transcative energy management tool for local ECs. In this work, the authors demonstrated the superaditivity of the derived coalitional game, by which it proved that the grand coalition is the best option for a given set of prosumers. In [21], a real case study was conducted in Austria, where a simple MILP formulation showed the benefits of adopting community structures. Privacy concerns have been also considered, for example, [22] proposed a hierarchichal framework for flexibility sharing in ECs, in which only net demand profiles are eefectively shared with other agents partaking in the community.

The references above propose analytical techniques for conducting the optimal planning or operation of ECs. Although these techniques are generally preferred because of their capability to reach the global optimum, other authors have explored the use of heuristic or metaheuristic approaches which are occasionally able to reduce the computational burden of the problem. Such is the case of the works developed by Liu et al. [23], where logic heuristic algorithms are considered for scheduling the community assets. Such approaches are based on logical decisions founded on heuristic criteria that usually lead to near-optimal solutions. On the other hand, the reference [24] uses metaheuristic techniques based on evolutionary algorithms to optimally allocate the commitment decisions among P2P transactions and other scheduling orders.

So far, all the references analysed consider deterministic conditions to determine the scheduling plan for the community. This assumption is clearly unreal and may lead to overoptimistic solutions. In real cases, ECs are operated under highly uncertain conditions. There are limited studies on uncertain modelling in ECs. Some of them propose stochastic approaches. Difficulties to assign probability distributions to uncertain parameters were addressed in [25] by developing a Markovian-based day-ahead decision process for ECs, where in thermal necessities were considered together with electricity consumption. The reference [26] dealt with heterogeneus risk-character of prosumers, for which a risk trading mechanism based on Arrow-Debreu securities. Within this framework, physical probabilities of scenarios are altered by introducing risk-aversion strategy of users, thus ensuring that the solution encountered lies within the conditional-value-at-risk. On the other hand, [27] proposes a holistic decision-making process for ECs encompassing day-ahead and intra-day scheduling. In [28], a stochastic bilevel approach was proposed for price-setting process in ECs incorporating collective storage systems.

Although stochastic programming is one of the most popular uncertainty models, its application may suppose intractability issues due to the size of the resulting problem. This issue is more evident when the problem is nonlinear [27], for which scenario reduction techniques can be applied [25]. To overcome the issues drawn by stochastic programs, the reference [29] proposed to use a simple interval algorithm based on confidence intervals on forecasted profiles rather than scenarios, while [30] relied on the use of information gap decision theory, thus reducing the complexity of the system.

The references analysed deal with isolated operation of communities, only considering the point of view of the EC operator, while the interaction with the distribution grid is neglected or oversimplified. Nevertheless, there exists some particular exceptions, like [31], where the stability of the grid is contemplated when sizing the capacity of the communities involving a large number of prosumers. On the ther hand, in [32] the figure of the DSO is included, considering interactions between this agent and the rest of the prosumers, which can still exchange energy through P2P mechanisms. Although including the network supposes an advance compared with other works, such references do not properly model uncertainties yet. While [31] is performed under deterministic conditions, [32] raises a simple Montecarlo-based approach to determine the reserve requirements for properly minimizing the effects of unknowns without explicitly modelling all the uncertainties involved in the problem.

1.3 - Gaps & contributions

To the best of our knowledge, dealing with multiple uncertainties in ECs is still an open topic. As reviewed above, the existing works mostly envisage stochastic approaches that present various significant drawbacks. The unique exception are the reference [29], where an iterative interval notation inspired in [33] was used, and [30], where information gap decision theory is considered to model the uncertainties associated with P2P sharing in communities. In this paper, we consider the same approach but including the figure of the DSO. In this regard, we develop a bi-level scheduling strategy for optimal cooperation among the DSO and ECs, involving DGs and customer-owned assets located in communities. The problem of determining the distribution energy prices, by which the communities can exchange energy with the grid, is also solved by proposing a Stackelberg-based algorithm. Moreover, the DN is explicitly modelled to account for bottelenecks or voltage issues. With this novel proposal, we aim to fill the major gaps encountered in the literature since, for the first time, a coordinated framework among DSO and ECs considering uncertainties through interval modelling is developed. The resulting MILP formulation is tractable, as demonstrated by extensive numerical simulation results on the IEEE 33-bus distribution system.

In the rest of this paper, Section 2 provides some preliminary ideas and concepts. Section 3 presents the mathematical formulation under deterministic conditions. Uncertainties are included via interval formulation in Section 4. Section 5 develops a Stackelberg-based approach for determining distributed energy prices. A case study is presented in Section 6. The paper is concluded with Section 7.

2 - Preliminaries

This article focuses on the optimal operation of DNs that incorporate ECs. In this task, different agents are involved posing different objectives and managing strategies. A summary of the different agents involved is depicted in Fig. 1, whose roles are further explained below:

- **DSO:** is responsible of operating distributed assets, including DGs and large-scale energy storage systems. This agent also operates the DN to which users are connected. It is assumed that the DSO determines the price under which energy transactions among the DN and the users are performed (distribution prices).
- **EC operator:** as commented, an EC is formed by a group of prosumers that are centrally operated by the EC operator. There is a variety of different control schemes for ECs [34]. In this paper, we assume cooperative ECs in which P2P transactions are performed solidary [18]. In this regard, the EC operator can manage local small-scale generators (rooftop PVs) and BESs together with controllable appliances (CAs) and electric vehicles (EVs). This paper assumes that the EC operator is also responsible of determining the P2P transactions among prosumers, thus adopting a coordinated management strategy [35]. The ECs can also exchange energy with the DN taking the prices fixed by the DSO (distribution prices).
- **Passive consumers:** this definition encompasses those users that are directly connected to the DN. However, in contrast to ECs, they are pure loads, and no local generation is available. In this sense, their role is limited to acquiring energy from the grid.

- **Transmission system operator (TSO)/retailer:** this agent owns or operates the utility grid to which the DN is connected and from which it can import/export energy. He sets the day-ahead dynamic price signals under which can exchange energy with the DN at convenience of the DSO.

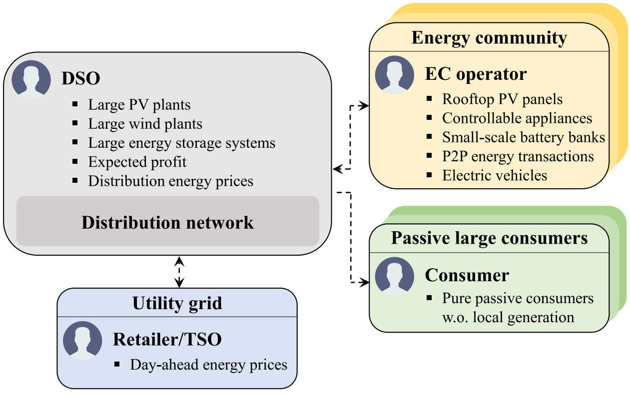

Fig. 1 - The different agents involved in DN operation

Fig. 2 sketches the timeline of the proposed coordinated scheduling strategy. Firstly, the retailer communicates to the DSO the day-ahead energy prices. This is a reasonable assumption since most retailers and utilities worldwide make publicly available their energy prices (purchasing and selling) over a 24-h time horizon [36]. Then, based on these prices, the DSO determines the distribution prices by adding his own profit. This process will be cleared through a developed Stackelberg-based procedure, which seeks the equilibrium point among the DSO and users (see Section 5). Finally, the scheduling program for the DN and ECs is established. This task is formulated as a bi-level optimization framework. In this framework, the scheduling plan of ECs is decided at the lower level, whereas the DSO establishes its program at the upper level.

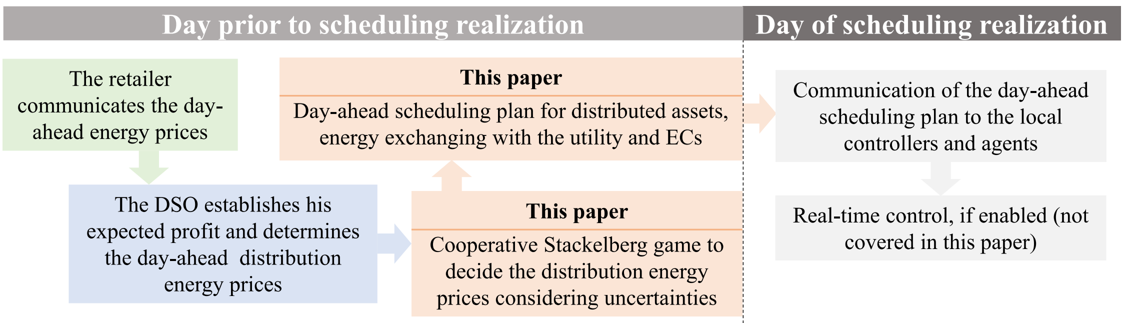

Fig. 2 - Timeline of the proposed coordinated scheduling strategy

3 - Deterministic problem

This section presents the mathematical formulation from a deterministic point of view. As commented, the scheduling strategy is arranged as a bi-level optimization framework where the ECs and DSO partake in a coordinated way. At the lower level, the ECs define their scheduling plan while the DSO reacts at the upper level setting the distribution prices as wel as deciding the scheduling strategy for the different distributed assets.

In this paper, we prefer a bi-level framework due to two reasons:

- The DSO and EC operators are different entities and therefore the amount of information exchanged between them should be limited.
- The EC scheduling plan is decided as a reaction to the distribution prices fixed by the DSO, which are at the same time a consequence of the scheduling plan performed by the DSO. So that the scheduling result of ECs must be performed *a posteriori*.

3.1 - Lower level: ECs scheduling

At the lower level, the scheduling plan of the communities is decided. EC operators usually perform this task, for which rooftop PV arrays, P2P transactions, small-scale BESs, domestic CAs, and EVs can be managed in a coordinated way among the prosumers in the community. In this regard, we deal here with a particular case of ECs in which P2P transactions among prosumers are performed without expecting a monetary counterpart. In other words, the different prosumers partaking in the community are keen to share resources by free. Note that this is a plausible assumptions in ECs, where the minimization of the collective bill is typically pursued. In this sense, sharing enegy through P2P exchanges leads to minimize the electricity bill and thus users may be keen on partaking in the community operation.

The objective of this level is to minimize the operating cost of each community, for which it is assumed that the distribution prices are known. Accordingly, this level reads as:

$$\left[\overline{p}_{c|t}^{DN,buy}, \overline{p}_{c|t}^{DN,sell}\right] \leftarrow \min_{\boldsymbol{x}_c^{EC}, \boldsymbol{u}_c^{EC}} F_c^{EC} = \Delta t \cdot \sum_{t \in \boldsymbol{\mathcal{T}}} \left\{ \pi_t^{DN,buy} \cdot p_{c|t}^{DN,buy} - \pi_t^{DN,sell} \cdot p_{c|t}^{DN,sell} \right\}; \forall c \in \boldsymbol{\mathcal{EC}} \quad (1)$$

Subject to:

$$p_{c|t}^{DN,buy} = \sum_{i \in \boldsymbol{\mathcal{P}}_c} \left\{ p_{i|t}^{DN,buy} \right\},\ p_{c|t}^{DN,sell} = \sum_{i \in \boldsymbol{\mathcal{P}}_c} \left\{ p_{i|t}^{DN,sell} \right\};\ \forall c \in \boldsymbol{\mathcal{EC}} \wedge t \in \boldsymbol{\mathcal{T}} \quad (2)$$

$$p_{i|t}^{DN,buy} + p_{i|t}^{PV} + p_{i|t}^{BES,dch} + p_{i|t}^{EV,dch} + \sum_{\substack{j \in \boldsymbol{\mathcal{P}}_c \\ j \neq i}} \left\{ p_{j \to i|t}^{P2P} \right\} = p_{i|t}^{DN,sell} + p_{i|t}^{NC} + p_{i|t}^{BES,ch} + p_{i|t}^{EV,ch} + \sum_{l \in \left\{ \substack{hot; \\ cool} \right\}} \left\{ p_{i|t}^{HVAC,l} \right\} + \sum_{a \in \left\{ \boldsymbol{\mathcal{A}}_i^I \cup \boldsymbol{\mathcal{A}}_i^{NI} \right\}} \left\{ u_{i|t}^a \cdot p_i^a \right\} + \sum_{\substack{j \in \boldsymbol{\mathcal{P}}_c \\ j \neq i}} \left\{ p_{i \to j|t}^{P2P} \right\};\ \forall i \in \boldsymbol{\mathcal{P}}_c \wedge c \in \boldsymbol{\mathcal{EC}} \wedge t \in \boldsymbol{\mathcal{T}} \quad (3)$$

$$p_{i \to j|t}^{P2P} - p_{j \to i|t}^{P2P} = 0; \forall i,j \in \boldsymbol{\mathcal{P}}_c \wedge c \in \boldsymbol{\mathcal{EC}} \wedge t \in \boldsymbol{\mathcal{T}} \quad (4)$$

$$p_{i|t}^{DN,l} \leq u_{i|t}^{DN,l} \cdot \overline{p}_i^{DN}; \forall i \in \boldsymbol{\mathcal{P}}_c \wedge c \in \boldsymbol{\mathcal{EC}} \wedge t \in \boldsymbol{\mathcal{T}} \wedge l \in \{buy; sell\} \quad (5)$$

$$u_{i|t}^{DN,buy} + u_{i|t}^{DN,sell} \leq 1; \forall i \in \boldsymbol{\mathcal{P}}_c \wedge c \in \boldsymbol{\mathcal{EC}} \wedge t \in \boldsymbol{\mathcal{T}} \quad (6)$$

$$\varepsilon_{i|t}^l = \varepsilon_{i|t-1}^l + \Delta t \cdot \left(\eta_i^{BES,ch} \cdot p_{i|t}^{l,ch} - \frac{p_{i|t}^{l,dch}}{\eta_i^{BES,dch}} \right);\ \forall i \in \boldsymbol{\mathcal{P}}_c \wedge c \in \boldsymbol{\mathcal{EC}} \wedge t \in \boldsymbol{\mathcal{T}} \backslash t > 1 \wedge l \in \{BES; EV\} \quad (7)$$

$$p_{i|t}^{l,m} \leq u_{i|t}^{l,m} \cdot \frac{\overline{\varepsilon}_i^l}{\mathrm{e2P}_i^l};\ \forall i \in \boldsymbol{\mathcal{P}}_c \wedge c \in \boldsymbol{\mathcal{EC}} \wedge t \in \boldsymbol{\mathcal{T}} \wedge l \in \{BES; EV\} \wedge m \in \{ch;\ dch\} \quad (8)$$

$$u_{i|t}^{l,ch} + u_{i|t}^{l,dch} \leq 1;\ \forall i \in \boldsymbol{\mathcal{P}}_c \wedge c \in \boldsymbol{\mathcal{EC}} \wedge t \in \boldsymbol{\mathcal{T}} \wedge l \in \{BES; EV\} \quad (9)$$

$$\varepsilon_{i|\boldsymbol{\mathcal{T}}[1]}^{BES} = \varepsilon_{i|\boldsymbol{\mathcal{T}}[\mathrm{end}]}^{BES} = \overline{\varepsilon}_i^{BES};\ \forall i \in \boldsymbol{\mathcal{P}}_c \wedge c \in \boldsymbol{\mathcal{EC}} \quad (10)$$

$$\varepsilon_{i|\boldsymbol{\Theta}_i^{EV}[1]}^{EV} = \varepsilon_i^{EV,0},\ \varepsilon_{i|\boldsymbol{\Theta}_i^{EV}[\mathrm{end}]}^{EV} = \overline{\varepsilon}_i^{EV};\ \forall i \in \boldsymbol{\mathcal{P}}_c \wedge c \in \boldsymbol{\mathcal{EC}} \quad (11)$$

$$u_{i|t}^{EV,l} = 0;\ \forall i \in \boldsymbol{\mathcal{P}}_c \wedge c \in \boldsymbol{\mathcal{EC}} \wedge t \notin \boldsymbol{\Theta}_i^{EV} \wedge l \in \{ch; dch\} \quad (12)$$

$$T_{i|t}^{Air,in} = \left(1 - \frac{\Delta t}{10^3 \cdot M_i^{Air,in} \cdot C^{Air} \cdot R_i^{Build}} \right) \cdot T_{i|t-1}^{Air,in} + \frac{\Delta t \cdot T_{i|t-1}^{Air,out}}{10^3 \cdot M_i^{Air,in} \cdot C^{Air} \cdot R_i^{Build}} + \frac{\Delta t \cdot \mathrm{COP}_i^{HVAC} \cdot \left(p_{i|t}^{HVAC,hot} - p_{i|t}^{HVAC,cool} \right)}{0.000277 \cdot M_i^{Air,in} \cdot C^{Air}};\ \forall i \in \boldsymbol{\mathcal{P}}_c \wedge c \in \boldsymbol{\mathcal{EC}} \wedge t \in \boldsymbol{\mathcal{T}} \backslash t > 1 \quad (13)$$

$$T_i^{HVAC,sp} - T_i^{HVAC,db} \leq T_{i|t}^{Air,in} \leq T_i^{HVAC,sp} + T_i^{HVAC,db};\ \forall i \in \boldsymbol{\mathcal{P}}_c \wedge c \in \boldsymbol{\mathcal{EC}} \wedge t \in \boldsymbol{\mathcal{T}} \quad (14)$$

$$p_{i|t}^{HVAC,l} \leq u_{i|t}^{HVAC,l} \cdot \overline{p}_i^{HVAC}; \forall i \in \boldsymbol{\mathcal{P}}_c \wedge c \in \boldsymbol{\mathcal{EC}} \wedge t \in \boldsymbol{\mathcal{T}} \wedge l \in \{hot; cool\} \quad (15)$$

$$u_{i|t}^{HVAC,hot} + u_{i|t}^{HVAC,cool} \leq 1; \forall i \in \boldsymbol{\mathcal{P}}_c \wedge c \in \boldsymbol{\mathcal{EC}} \wedge t \in \boldsymbol{\mathcal{T}} \quad (16)$$

$$T_{i|\mathcal{T}[1]}^{Air,in} = T_{i|\mathcal{T}[\text{end}]}^{Air,in} = T_i^{HVAC,sp};\ \forall i \in \mathcal{P}_c \wedge c \in \mathcal{EC} \tag{17}$$

$$\sum_{t\in\boldsymbol{\Theta}_i^a}\left\{u_{i|t}^a\right\} = \mathrm{DC}_i^a; \forall i \in \mathcal{P}_c \wedge c \in \mathcal{EC} \wedge a \in \left\{\mathcal{A}_i^I \cup \mathcal{A}_i^{NI}\right\} \tag{18}$$

$$u_{i|t}^a - u_{i|t-1}^a = on_{i|t}^a - off_{i|t}^a; \forall i \in \mathcal{P}_c \wedge c \in \mathcal{EC} \wedge t \in \mathcal{T} \backslash t > 1 \wedge a \in \mathcal{A}_i^{NI} \tag{19}$$

$$\sum_{t\in\boldsymbol{\Theta}_i^a}\left\{on_{i|t}^a\right\} = 1; \forall i \in \mathcal{P}_c \wedge c \in \mathcal{EC} \wedge a \in \mathcal{A}_i^{NI} \tag{20}$$

where $\boldsymbol{x}_c^{EC}$ and $\boldsymbol{u}_c^{EC}$ are the vectors of continuous and binary decision variables for the c^{th} EC, respectively (see Appendix A). By minimizing the energy cost of the community (1), the energy that must be imported from the DN is obtained ($\overline{p}_{c|t}^{DN,buy}$), together with the maximum exportable power ($\overline{p}_{c|t}^{DN,sell}$). These two values are calculated as in (2) and sent to the DSO, who uses this information to determine his own scheduling plan (see Section 3.2).

The power balance of the community is established in (3). This balance ensures that generation meets demand any time instant taking into account P2P exchanges among prosumers, which can be conceived as virtual loads/generators depending whether the prosumer exports/imports power. On the other hand, (4) ensures that the power exported from the i^{th} prosumer to the j^{th} prosumer is equal to the power that the j^{th} prosumer imports from the i^{th} prosumer [12], thus ensuring equilibrium in P2P exchanges. Moreover, (5) establishes limits in the importable/exportable power, assuming that the DSO imposes a bound of the energy flows to avoid surpass thermal limit of branches or equipment, while (6) avoids simultaneous purchases and sales, as customary [29].

Equation (7) models the instantaneous state-of-charge (SOC) of storage devices (BESs and EVs) as a function of the SOC at the previous time step and the energy exchanged. On the other hand, (8) fixes the rated power of batteries considering the total capacity and energy-to-power ratio [37], whereas (9) avoids simultaneous charging-discharging of storage devices. Since (7) is not defined at $t = 1$, the initial SOC of stationary batteries is fixed by (10). As customary, the initial SOC is set equal to the total capacity and, in order to keep the model coherent, the final SOC is fixed equal to the initial in (8) [38]. In contrast, the initial SOC of EVs is considered a random parameter given by $\varepsilon_i^{EV,0}$, while we assume that users are keen to get the vehicle fully charged at tits departure time [39], as said (11). Lastly, it is worth noting that EVs can only be scheduled qhen they are pluuged, which is endured by (12) where the EV time window is given by the set $\boldsymbol{\Theta}_i^{EV}$.

The indoor temperature of each home is determined by (13), which is a function of the outdoor temperature and the action of heating-ventilation-air conditioner (HVAC) devices. This model is derived from the differential equations that model heat transfer in buildings, which can be linearized on the basis of plausible assumptions [30]. Equation (14) establishes thermal comfort by limiting the indoor temperature to comfortable bounds. In such limits, deadband terms are included to avoid frequent operation of HVAC devices. Equation (15) upper bounds the HVAC consumption to rated values while (16) establishes complementarity in heating and cooling modes. Similar to batteries, equation (17) completes the HVAC model by fixing the initial and final values of the indoor temperature, since (13) is not defined at $t = 1$ [39].

Finally, the set of constraints (18)-(20) models the CAs, which are divided into interruptible and non-interruptible [40]. While the former can be interrupted at convenience, the latter must complete their duty cycles over a continuous operation mode. In addition, we consider that CAs cannot be scheduled feeely and home inhabitants eatsblish predefined time windows within wwhich the operation of appliances can be shifted. These time windows (given by $\boldsymbol{\Theta}_i^a$) aim at modelling the different users' preferences on the operation of CAs. According to these premises, (18) ensures that duty cycles are completed within pre-established time windows, while the equations (19) and (20) are particular to non-interruptible appliances, establishing continuity and ensuring a unique activation order, respectively [40].

3.2 - Upper level: DN scheduling

Once the DSO receives information from the retailer (day-ahead energy prices), the day-ahead scheduling strategy for distributed assets (i.e., DGs and large-scale BESs) can be performed. The DSO aims to minimize the operating cost of the DN while satisfying the demand of the connected users (i.e., ECs and passive consumers). To this end, the retailer communicates the day-ahead energy prices, which are subjected to uncertainty. As a consequence of the decisions taken at this level, the distribution prices are cleared (see Section 5). Note that distribution prices are not actually decided at this level rather than the scheduling plan for the distributed assets. The different distribution prices are online calculated by the Stackelberg-game framework developed in Section 5. In this sense, distribution prices are taken as parameters at this level.

Thus, the upper level can be formulated as follows:

$$\min_{\boldsymbol{x}^{DN},\boldsymbol{u}^{DN}} F^{DSO} = \Delta t \cdot \sum_{t\in\mathcal{T}}\Big\{\pi_t^{UG,buy}\cdot p_t^{UG,buy} - \pi_t^{UG,sell}\cdot p_t^{UG,sell} + \sum_{c\in\mathcal{EC}}\Big\{\pi_t^{DN,sell}\cdot p_{c|t}^{DN,sell} - \pi_t^{DN,buy}\cdot p_{c|t}^{DN,buy}\Big\} - \sum_{c\in\mathcal{C}}\Big\{\pi_t^{DN,buy}\cdot p_{c|t}^{DN,buy}\Big\}\Big\} \tag{21}$$

Subject to:

$$p_t^{UG,buy} + \sum_{g\in\mathcal{G}}\{p_{g|t}\} + \sum_{c\in\mathcal{EC}}\{p_{c|t}^{DN,sell}\} + \sum_{s\in\mathcal{S}}\{p_{s|t}^{BES,dch}\} = p_t^{UG,sell} + \sum_{s\in\mathcal{S}}\{p_{s|t}^{BES,ch}\} + \sum_{c\in\{\mathcal{EC}\cup\mathcal{C}\}}\Big\{\overline{p}_{c|t}^{DN,buy}\Big\}; \forall t\in\mathcal{T} \tag{22}$$

$$p_{c|t}^{DN,sell} \le \overline{p}_{c|t}^{DN,sell}; \forall c\in\mathcal{EC}\wedge t\in\mathcal{T} \tag{23}$$

$$p_t^{UG,l} \le u_t^{UG,l}\cdot\overline{p}^{UG}; \forall t\in\mathcal{T}\wedge l\in\{buy; sell\} \tag{24}$$

$$u_t^{UG,buy} + u_t^{UG,sell} \le 1; \forall t\in\mathcal{T} \tag{25}$$

$$p_{g|t} \le \mathbb{E}[p_{g|t}]; \forall g\in\mathcal{G}\wedge t\in\mathcal{T} \tag{26}$$

$$P_{b+1|t} = P_{b|t} + \sum_{c\in\{\mathcal{EC}_b\cup\mathcal{C}_b\}}\Big\{\overline{p}_{c|t}^{DN,buy}\Big\} + \sum_{s\in\mathcal{S}_b}\{p_{s|t}^{BES,ch}\} - \sum_{g\in\mathcal{G}_b}\{p_{g|t}\} - \sum_{c\in\mathcal{EC}_b}\{p_{c|t}^{DN,sell}\} + \sum_{s\in\mathcal{S}_b}\{p_{s|t}^{BES,dch}\}; \forall b\in\mathcal{B}\backslash b<|\mathcal{B}|\wedge t\in\mathcal{T} \tag{27}$$

$$V_{b+1|t} = V_{b|t} - \frac{r_b\cdot P_{b|t}}{V_{\mathcal{B}[1]|t}}; \forall b\in\mathcal{B}\backslash b<|\mathcal{B}|\wedge t\in\mathcal{T} \tag{28}$$

$$-\overline{P}_b \le P_{b|t} \le \overline{P}_b; \forall b\in\mathcal{B}\wedge t\in\mathcal{T} \tag{29}$$

$$\underline{V}_b \le V_{b|t} \le \overline{V}_b; \forall b\in\mathcal{B}\wedge t\in\mathcal{T} \tag{30}$$

$$\varepsilon_{s|t}^{BES} = \varepsilon_{s|t-1}^{BES} + \Delta t\cdot\left(\eta_s^{BES,ch}\cdot p_{s|t}^{BES,ch} - \frac{p_{s|t}^{BES,dch}}{\eta_s^{BES,dch}}\right); \ \forall s\in\mathcal{S}\wedge t\in\mathcal{T}\backslash t>1 \tag{31}$$

$$p_{s|t}^{BES,m} \le u_{s|t}^{BES,m}\cdot\frac{\overline{\varepsilon}_s^{BES}}{\mathrm{e2P}_s^{BES}}; \ \forall s\in\mathcal{S}\wedge t\in\mathcal{T}\wedge m\in\{ch; dch\} \tag{32}$$

$$u_{s|t}^{BES,ch} + u_{s|t}^{BES,dch} \le 1; \ \forall s\in\mathcal{S}\wedge t\in\mathcal{T} \tag{33}$$

$$\varepsilon_{s|\mathcal{T}[1]}^{BES} = \varepsilon_{s|\mathcal{T}[\mathrm{end}]}^{BES} = \overline{\varepsilon}_s^{BES}; \ \forall s\in\mathcal{S} \tag{34}$$

where $\boldsymbol{x}^{DN}$ and $\boldsymbol{u}^{DN}$ collect the continuous and binary decision variables of the upper level, respectively (see Appendix A). The objective function (21) encompasses cost-revenue balances with the utility grid and ECs, determined by energy exchanged with such users as well as revenues obtained from selling energy to passive consumers.

The power balance (22) ensures that consumers' demand is fully satisfied, taking into account self-generation and storage via DGs and distributed BESs, respectively. This equation also includes the energy exchanged with the utility grid. However, the DSO can decide whether exportable power from ECs is used or not, as said (23). In this sense, ECs communicate their maximum exportable power, which is calculated by solving the lower level. Nevertheless, this information supposes a limit in the exportable power that is available at the DSO's convenience, who can decide to exploit such energy or not. On the other hand, (24) and (25) limit the power exchanged with the utility grid and avoid simultaneous imports and exports, respectively. In this regard, we assume that the retailer and TSO can be different entities. Indeed, while the retailer communicates prices, the TSO concers about operatibility of the utility grid and can impose limits in importable/exportable power in consequence.

We assume that DGs are based on rewable sources. As such, their potential generation is uncertain and it relies on weather parameters such as solar irradiance and wind speed. In this sense, (26) limits the maximum DG exportable power to expected values, whose inherent uncertainty is modelled in Section 4 using interval notation. Note that dispatchable DGs can be easily incorporated just by modifying (26) to include rated powers instead of expected values, as in [41].

Furthermore, (27) and (28) model the network using the LinDistFlow equations. It is worth noting that other power flow models exist based on exact trigonometric equations or second oerder exact approsimations. Nonetheless, such models rely on nonlinear equations. In this sense, we prioritize the tractability of the developed formulation, for which we believe essential keep the linearity of equations. In this regard, whose usefulness and accuracy of the LinDistFlow model has been well-proved [42]. The network model is completed by (29) and (30), which establish limits for power flows through branches and nodal voltages, respectively. Finally, the set of constraints (31)-(34) models the distributed BESs, which are analogue to (7)-(10).

4 - Interval-based procedure to include uncertainties

Energy management in active DNs is subjected to multiple uncertainties. In this section, we modifiy the bi-level operational model described in Section 3 to accommodate a variety of uncertain parameters. In this regard, we assume that uncertainties are only concerned at the upper level since at this stage uncertainties from all the communities are aggregated, being so more easily manageable.

Uncertainties modelling in active DNs has attracted huge attention recently. In this field one can finf a number of scenario-based [43] or robust approaches [44] in the literature. Regarding ECs, stochastic approaches have been successfully applied in [27]. Nonetheless, as commented in the Introduction, these techniques pose various drawbacks. In this regard, we prefer using robust techniques, among which one can find robust reformulations [45], Information Gap Decision Theory approximations [46], or interval-based problems [47]. This paper uses interval-based procedures, assuming that related uncertainties can be predicted with acceptable accuracy.

In their original form, interval problems may be computationally unaffordable due to complementarity constraints that must be added to convert the original optimization framework into a single-level structure [47]. To overcome this issue, [33] proposed an iterative procedure, which has also been applied to other related problems [48]. This procedure is iteratively performed in three stages, as summarized in the flowchart in Fig. 3. The convergence criterion is given by

$$\frac{\left|F_{k_1}^{DSO}-F_{k_1-1}^{DSO}\right|}{F_{k_1}^{DSO}} \leq tol_1 \tag{35}$$

where the subscript denotes the k_1^{th} iteration of the iterative procedure. In this paper, the tolerance threshold is 0.01 [33]. Subsequent sections are devoted to applying the procedure described in Fig. 3 to the problem presented in Section 3.

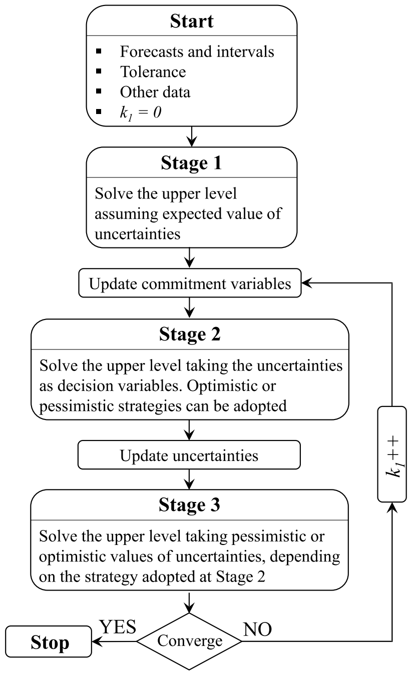

Fig. 3 - Flowchart of the iterative procedure to consider uncertainties via interval optimization

4.1 - Stage 1: deterministic problem

The first stage focuses on solving the upper level (21)-(34) under deterministic conditions, i.e., assuming expected (forecasted) values of uncertainties. In this case, the commitment result of assets is stored, thus defining this stage as

$$\boldsymbol{u}^{DN,*} \rightarrow \underset{\boldsymbol{x}^{DN},\boldsymbol{u}^{DN}}{\operatorname{argmin}} F^{DSO}(\mathbb{E}[\boldsymbol{\Omega}]) \tag{36}$$

Subject to: (22)-(34)

4.2 - Stage 2: interval-based problem

This stage seeks for favourable or unfavourable values of uncertainties depending on whether an optimistic or pessimistic operational strategy is adopted. To this end, involved uncertainties (i.e., utility energy prices, renewable generation, and demand) are considered as decision variables, allowing them to vary within predefined confidence intervals described in (37).

$$\mathbb{E}[\omega] - \xi \cdot \Delta\omega^{\downarrow} \leq \omega \leq \mathbb{E}[\omega] + \xi \cdot \Delta\omega^{\uparrow}; \forall \omega \in \boldsymbol{\Omega} \tag{37}$$

The constraint (37) allows to model the generic uncertainty ω as an interval number of the form $\omega \in \left[\mathbb{E}[\omega] - \Delta\omega^{\downarrow}, \mathbb{E}[\omega] + \Delta\omega^{\uparrow}\right]$. In (37), $\xi \in [0,1]$ is the so-called uncertain level, which allows tuning the level of the considered confidence intervals [48]. Moreover, considering energy prices as variables produces nonlinearity by adding bi-linear terms in (21), which may become the problem non-convex. To solve this issue, we use the linearization technique defined in [49], which is described by the constraints (38)-(49). This technique allows converting the original quadratic problem into a manageable MILP.

$$z_t^{UG,l} = \pi_t^{UG,l} \cdot p_t^{UG,l}; \forall t \in \boldsymbol{\mathcal{T}} \wedge l \in \{buy;\ sell\} \tag{38}$$

$$\pi_t^{UG,l} \approx \langle \tilde{\pi}_{t|i}^{UG,l} \rangle;\ \forall t \in \boldsymbol{\mathcal{T}} \wedge i \in \{1,2,\dots,n\} \wedge l \in \{buy;\ sell\} \tag{39}$$

$$\zeta_{t|i}^{UG,l} = \tilde{\pi}_{t|i}^{UG,l} - \tilde{\pi}_{t|i-1}^{UG,l};\ \forall t \in \boldsymbol{\mathcal{T}} \wedge i \in \{1,2,\dots,n\} \wedge l \in \{buy;\ sell\} \tag{40}$$

$$\pi_t^{UG,l} = \sum_{i=1}^{i=n}\left\{\varphi_{t|i}^{UG,l} \cdot \tilde{\pi}_{t|i-1}^{UG,l} + \delta\tilde{\pi}_{t|i}^{UG,l}\right\};\ \forall t \in \boldsymbol{\mathcal{T}} \wedge l \in \{buy;\ sell\} \tag{41}$$

$$\varphi_{t|i}^{UG,l} \in \mathbb{SOS}1;\ \forall t \in \boldsymbol{\mathcal{T}} \wedge i \in \{1,2,\dots,n\} \wedge l \in \{buy;\ sell\} \tag{42}$$

$$0 \leq \delta\tilde{\pi}_{t|i}^{UG,l} \leq \zeta_{t|i}^{UG,l} \cdot \varphi_{t|i}^{UG,l};\ \forall t \in \boldsymbol{\mathcal{T}} \wedge i \in \{1,2,\dots,n\} \wedge l \in \{buy;\ sell\} \tag{43}$$

$$p_t^{UG,l} = \sum_{i=1}^{i=n}\left\{\delta p_{t|i}^{UG,l}\right\};\ \forall t \in \boldsymbol{\mathcal{T}} \wedge l \in \{buy;\ sell\} \tag{44}$$

$$0 \leq \delta p_{t|i}^{UG,l} \leq \overline{p}^{UG};\ \forall t \in \boldsymbol{\mathcal{T}} \wedge i \in \{1,2,\dots,n\} \wedge l \in \{buy;\ sell\} \tag{45}$$
$$z_t^{UG,l} = \sum_{i=1}^{i=n}\left\{\tilde{\pi}_{t|i-1}^{UG,l} \cdot \delta p_{t|i}^{UG,l}\right\} + \delta z_t;\ \forall t \in \boldsymbol{\mathcal{T}} \wedge l \in \{buy;\ sell\} \tag{46}$$
$$\delta z_t \geq \sum_{i=1}^{i=n}\left\{\zeta_{t|i}^{UG,l} \cdot \delta p_{t|i}^{UG,l}\right\} + \overline{p}^{UG} \cdot \sum_{i=1}^{i=n}\left\{\delta\tilde{\pi}_{t|i}^{UG,l} - \zeta_{t|i}^{UG,l} \cdot \varphi_{t|i}^{UG,l}\right\};\ \forall t \in \boldsymbol{\mathcal{T}} \wedge l \in \{buy;\ sell\} \tag{47}$$
$$\delta z_t \leq \overline{p}^{UG} \cdot \sum_{i=1}^{i=n}\left\{\delta\tilde{\pi}_{t|i}^{UG,l}\right\};\ \forall t \in \boldsymbol{\mathcal{T}} \wedge l \in \{buy;\ sell\} \tag{48}$$
$$\delta z_t \leq \sum_{i=1}^{i=n}\left\{\zeta_{t|i}^{UG,l} \cdot \varphi_{t|i}^{UG,l}\right\};\ \forall t \in \boldsymbol{\mathcal{T}} \wedge l \in \{buy;\ sell\} \tag{49}$$

where the δ's define continuous variables that measure the deviation of a variable with respect to its grid-point in its piecewise representation ($\langle * \rangle$), which are denoted by ($\tilde{*}$); and φ is a special ordered set 1 ($\mathbb{SOS}1$) binary variable. Indeed, the set of constraints above allows representing the nonlinear product $\pi \cdot p$ by the dummy linear variable z, which is calculated using piecewise representation of the energy prices and additional constraints for describing the behavior of the bi-linear product as a function of the value of the two variables involved.

In this way, Stage 2 can be fully described as follows:

$$\begin{cases} \boldsymbol{\Omega}^{pes} \rightarrow \underset{\boldsymbol{x}^{DN},\boldsymbol{\Omega},\boldsymbol{\Psi}}{\operatorname{argmax}} F^{DSO}(\boldsymbol{u}^{DN,*}) \\ \boldsymbol{\Omega}^{opt} \rightarrow \underset{\boldsymbol{x}^{DN},\boldsymbol{\Omega},\boldsymbol{\Psi}}{\operatorname{argmin}} F^{DSO}(\boldsymbol{u}^{DN,*}) \end{cases} \tag{50}$$

Subject to: (22)-(34), (37)-(49)
where $\boldsymbol{\Psi}$ is the vector collecting the auxiliar variables for the formulation (38)-(49) (see Appnedix). Note that Stage 2 varies if the assumed strategy is pessimistic or optimistic. In (50), the objective function is maximized in the former chase or minimized otherwise. It has been proved that this approach leads to calculating favourable or unfavourable profiles of uncertainties depending on the strategy adopted (optimistic or pessimistic, respectively) [48].

4.3 - Stage 3: adjustment problem

Finally, the problem is solved again, but assuming the value of uncertainties calculated at Stage 2, as follows:

$$\boldsymbol{u}^{DN,*} \rightarrow \underset{\boldsymbol{x}^{DN},\boldsymbol{u}^{DN}}{\operatorname{argmin}} F^{DSO}\left(\boldsymbol{\Omega}^{l}\right);\ l = pes \vee opt \tag{51}$$

Subject to: (22)-(34)

5 - Determination of distribution prices

After performing the developed optimization model described in sections 3 and 4, the scheduling plan for the distributed and community assets is decided for fixed distribution prices. However, we have not discussed yet how these prices are calculated. To this end, a Stackleberg-game framework is developed in this section, which is executed just after the DSO receives price signals from the retailer. This way, the scheduling plan for distributed assets can be performed under known prices and communities can react in consequence.

Determining the distribution prices is not a trivial task for DSOs. The DSO aims to obtain revenue as a service provider. In other words, the DSO aims at obtaining a profit, which is defined by the parameter $\lambda \geq 0$, so that distribution prices can be rewritten as a function of the utility ones, as follows:

$$\pi_t^{DN,buy} = (1+\lambda) \cdot \pi_t^{UG,buy}, \pi_t^{DN,sell} = (1-\lambda) \cdot \pi_t^{UG,sell};\ \forall t \in \boldsymbol{\mathcal{T}} \tag{52}$$

However, the profit should not be excessively high in order to ensure the welfare of users. Otherwise, they could be discouraged from importing energy from the DN recurring to other alternatives (e.g., incrementing their level of self-supplying). This problem is described as a Stackelberg-game framework (see Appendix B), whose objective is determining the optimal profit that ensures the collective welfare (namely λ^*). Stackelberg games describe a leader with one or more followers (participants), strategies, and benefits. Generally, there are two approaches to solve Stackelberg games. Firstly, KKT-based procedures can be used, leading to bi-level structures that must be converted to single-level problems [50]. As commented earlier, this approach may lead to unaffordable computational efforts. To solve this issue, metaheuristic-based routines have been also proposed [51]. However, this approach would require solving the iterative procedure in Fig. 3 many times, leading to a very complex and computationally costly procedure. To solve such issues, a simple bisection algorithm has been proposed based on [52], which is described below.

Firstly, it is necessary to define the game structure formally. For the particular case here concerned, the following Stackelberg game is defined to estimate the optimal profit.

$$\lambda^* \leftarrow \Phi = \left\{ \begin{matrix} \{\mathrm{DSO} \cup \boldsymbol{\mathcal{EC}} \cup \boldsymbol{\mathcal{C}}\} \\ \lambda;\ \left\{\overline{p}_{c|t}^{DN,buy}, \overline{p}_{c|t}^{DN,sell};\ \forall c \in \boldsymbol{\mathcal{EC}} \wedge t \in \boldsymbol{\mathcal{T}}\right\} \\ \Xi[\mathrm{DSO}];\ \Xi[\boldsymbol{\mathcal{EC}} \cup \boldsymbol{\mathcal{C}}] \end{matrix} \right\} \quad (53)$$

In (53), the DSO and users (ECs and passive consumers) are the participants, being leaded by the DSO, as sketched in Fig. 4. For a given a profit, the ECs can respond by adjusting their consumption profile so that the strategy is given by the profit and net demand of the ECs, assuming that passive consumers are inelastic loads. Finally, the benefits are here described by fitness functions given by

$$\Xi[\cdot] = \frac{f[\cdot] - \underline{f}[\cdot]}{\overline{f}[\cdot] - \underline{f}[\cdot]} \quad (54)$$

where

$$\begin{cases} f[\mathrm{DSO}] = F^{DSO} \\ f[\boldsymbol{\mathcal{EC}} \cup \boldsymbol{\mathcal{C}}] = \sum_{c \in \boldsymbol{\mathcal{EC}}}\{F_c^{EC}\} + \sum_{c \in \boldsymbol{\mathcal{C}}}\{F_c^{C}\} \end{cases} \quad (55)$$

Fig. 4 - Sketch of the Stackelberg-based mechanism to determine the distribution prices

As seen in (55), the fitness functions of each participant are described by their operating costs, while (54) is introduced to range the values of f's within $[0,1]$ and thus facilitating the comparison between fitness functions. The upper and lower bound of costs in (54) can be calculated by establishing an arbitrarily high profit $\overline{\lambda}$ and its minimum assumable value (i.e., $\lambda = 0$), as follows:

$$\begin{cases} \overline{f}[\mathrm{DSO}] = F^{DSO}(\lambda = 0);\ \underline{f}[\boldsymbol{\mathcal{EC}} \cup \boldsymbol{\mathcal{C}}] = \sum_{c \in \boldsymbol{\mathcal{EC}}}\{F_c^{EC}(\lambda = 0)\} + \sum_{c \in \boldsymbol{\mathcal{C}}}\{F_c^{C}(\lambda = 0)\} \\ \underline{f}[\mathrm{DSO}] = F^{DSO}(\lambda = \overline{\lambda});\ \overline{f}[\boldsymbol{\mathcal{EC}} \cup \boldsymbol{\mathcal{C}}] = \sum_{c \in \boldsymbol{\mathcal{EC}}}\{F_c^{EC}(\lambda = \overline{\lambda})\} + \sum_{c \in \boldsymbol{\mathcal{C}}}\{F_c^{C}(\lambda = \overline{\lambda})\} \end{cases} \quad (56)$$

The idea behind the formulation above is depicted in Fig. 5. It is reasonable to think that the fitness function of users will value 1 when $\overline{\lambda}$ is taken, while the fitness function of the DSO will take 0 at this point. At the other extreme (i.e., $\lambda = 0$), the fitness functions of the participants will take their opposite values (1 in the case of the DSO and 0 for the users). Therefore, as seen in Fig. 5, it is clear that both fitness functions cross at some point between $\lambda = 0$ and $\lambda = \overline{\lambda}$. According to the market theory [53], this point corresponds to the maximization of the collective welfare and, therefore, with the value of λ^*. Indeed, by observing Fig. 5 it is clear that λ^* corresponds to the point where all the participants achieve their maximum welfare, since at this point any of them can improve their fitness function without deteriorating others. This sentence holds if we assume that fitness functions are continuously increasing/decreasing within $[0, \overline{\lambda}]$, which is perfectly plausible since the fitness functions used in this paper correspond to energy costs, which are expected to be directly impacted by the profit λ (this idea has been confirmed by empirical evidences).

To estimate the value of λ^*, we develop a simple bisection algorithm which is summarized in the following points:

1. Set $k_2 = 0$, start with $\lambda_0 = \overline{\lambda}/2$ and solve the optimization problem subjected to uncertainties.
2. If $\Xi[\text{DSO}] > \Xi[\boldsymbol{\mathcal{EC}} \cup \boldsymbol{\mathcal{C}}]$ then define $\varpi = [0, \lambda_{k_2}]$, else $\varpi = [\lambda_{k_2}, \overline{\lambda}]$.
3. Set $\lambda_{k_2+1} = \frac{\varpi[2]-\varpi[1]}{2}$ and check the convergence criteria (57)

$$|\lambda_{k_2} - \lambda_{k_2+1}| \leq tol_2 \tag{57}$$

   where $tol_2 = 0.01$ in this paper.
4. If (57) is met, then $\lambda^* = \lambda_{k_2+1}$ and stop, else $k_2 = k_2 + 1$ and go to step 5.
5. Solve the optimization problem subjected to uncertainties. If $\Xi[\text{DSO}] > \Xi[\boldsymbol{\mathcal{EC}} \cup \boldsymbol{\mathcal{C}}]$ then define $\varpi = [\lambda_{k_2-1}, \lambda_{k_2}]$, else $\varpi = [\lambda_{k_2}, \lambda_{k_2-1}]$. Go to Step 3.

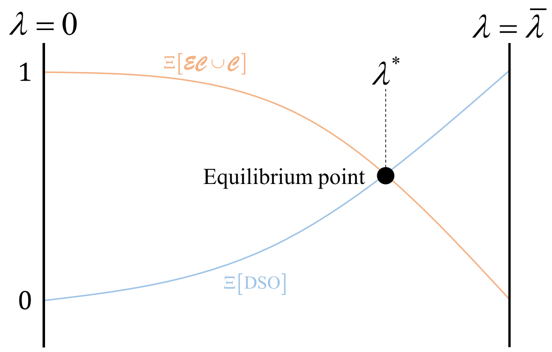

Fig. 5 - Illustrative representation of the equilibrium point (λ^*) as calculated using the developed Stackelberg-based bisection procedure

Empirical evidences demonstrate that the developed bisection algorithm usually converges after 3-4 iterations if $\overline{\lambda} \approx 0.10$, resulting in an assumable computational burden. Note that the developed bi-section mechanism assumes that distribution prices follow the same profile that prices fixed by the TSO (utility prices), which is perfectly plausible.

6 - Case study

6.1 - Case study data

This section presents a case study on the modified IEEE 33-bus network, as shown in Fig. 6. The original network, whose data can be found in [54], has been modified to include 10 ECs together with 2 PV plants, 3 wind farms, 2 storage systems, and 6 passive consumers. Fig. 7 reports the expected passive demands and renewable potential from the generators connected to the network, while Fig. 8 plots the expected utility prices. Both storage banks connected to the network have a capacity of 1000 kWh with 95 % efficiency [37], an energy-to-power ratio of 2-h [37], and an 80 % depth-of-discharge. The data in Figs. 7 and 8 are generated based on real databases. In particular, weather parameters namely solar irradiance, temperature and wind speed correspond to real profiles observed at Virgin Islands (U.S.) in 2016 [55]. On the other hand, demand corresponding to passive consumers was adapted to real consumption profiles observed at La Palma Island (Spain) in 2016 [56]. Finally, energy prices correspond to real-time prices for PJM Fe Ohio, also in 2016 [57]. To account for uncertainties, 20 % confidence intervals are established on the expected profiles. The resulting MILP problem described in previous sections is solved with a 30-min resolution, coded under Matlab R2021a. This computational arrangement results very suitable for the developed optimization model. Note that current version of Matlab offers a friendly problem-oriented coding for optimization problems, in which MILP formulations can be accommodated easily. Such coding environment serves as interface for the applicability of advanced solvers like Gurobi [58]. Moreover, Matlab allows to easily implement iterative routines and repeatedly calling different optimization problems as the algorithm advances, resulting very applicable for the methodology described here and facilitate data exchanging among the different steps of the algorithm.

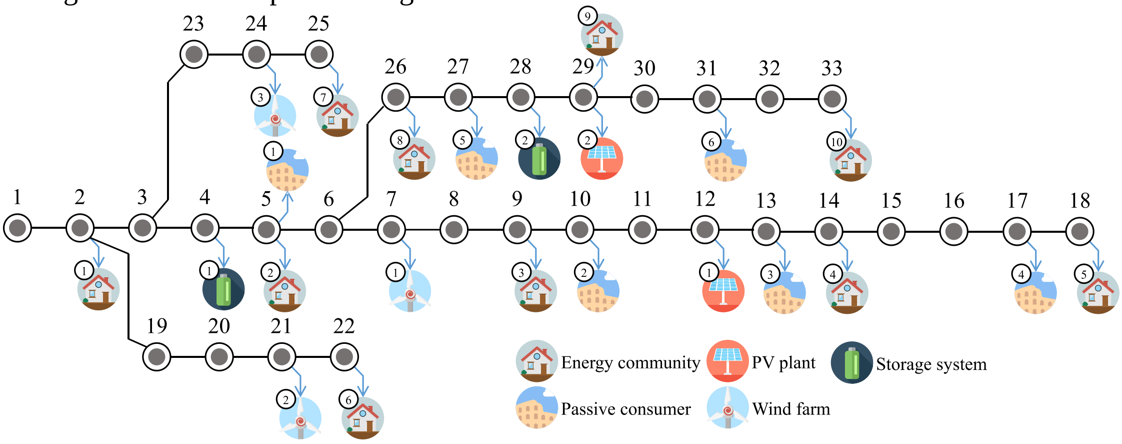

Fig. 6 - The modified IEEE 33-bus network used in simulations

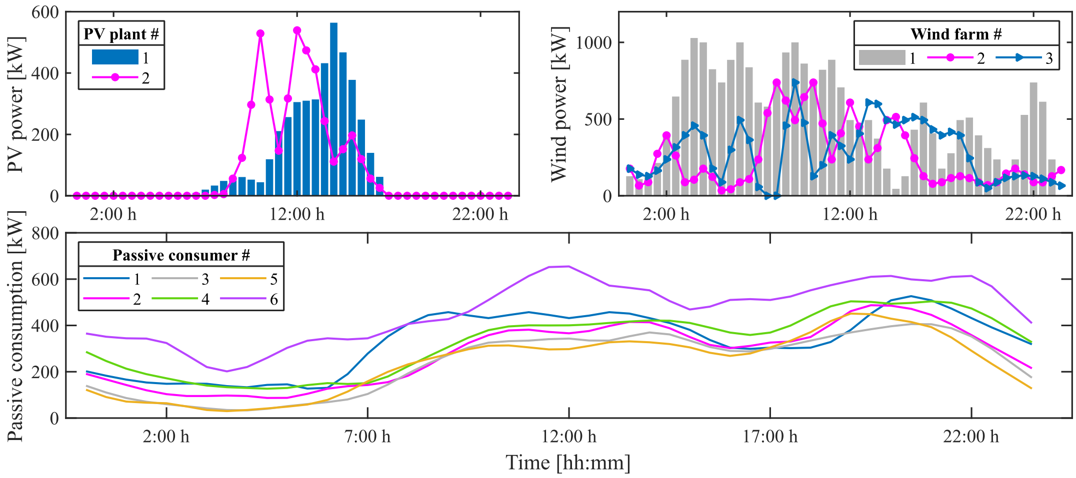

Fig. 7 - Expected PV and wind generation (top) and passive consumption (bottom)

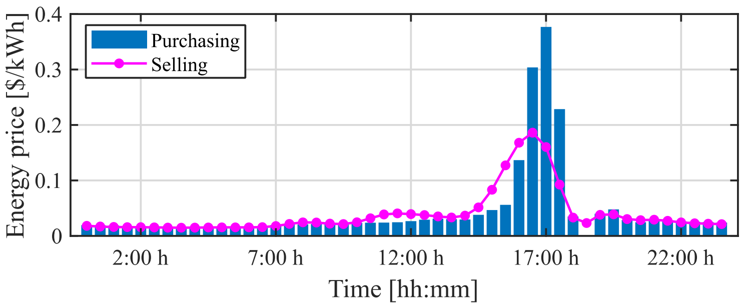

Fig. 8 - Expected energy prices for energy exchanging with the utility grid

Fig. 9 presents the expected non-controllable demand and PV generation in ECs (taking individual data for each prosumer within the community). The non-controllable demand has been taken from [59], which extracts the representative profiles following the methodology in [39]. Likewise, solar irradiance has been extracted from [55]. In this case, it is assumed that all the prosumers in a community receives the same irradiance because of their proximity, while outdoor temperature is the same as in [60]. With these data and typical PV panels rated power between

0.25-2.5 kWp, the PV profiles in Fig. 9 were constructed. The data regarding domestic assets and appliances were generated similarly by taking typical parameters reported in the literature (e.g. [39]). Table 1 summarizes these data.

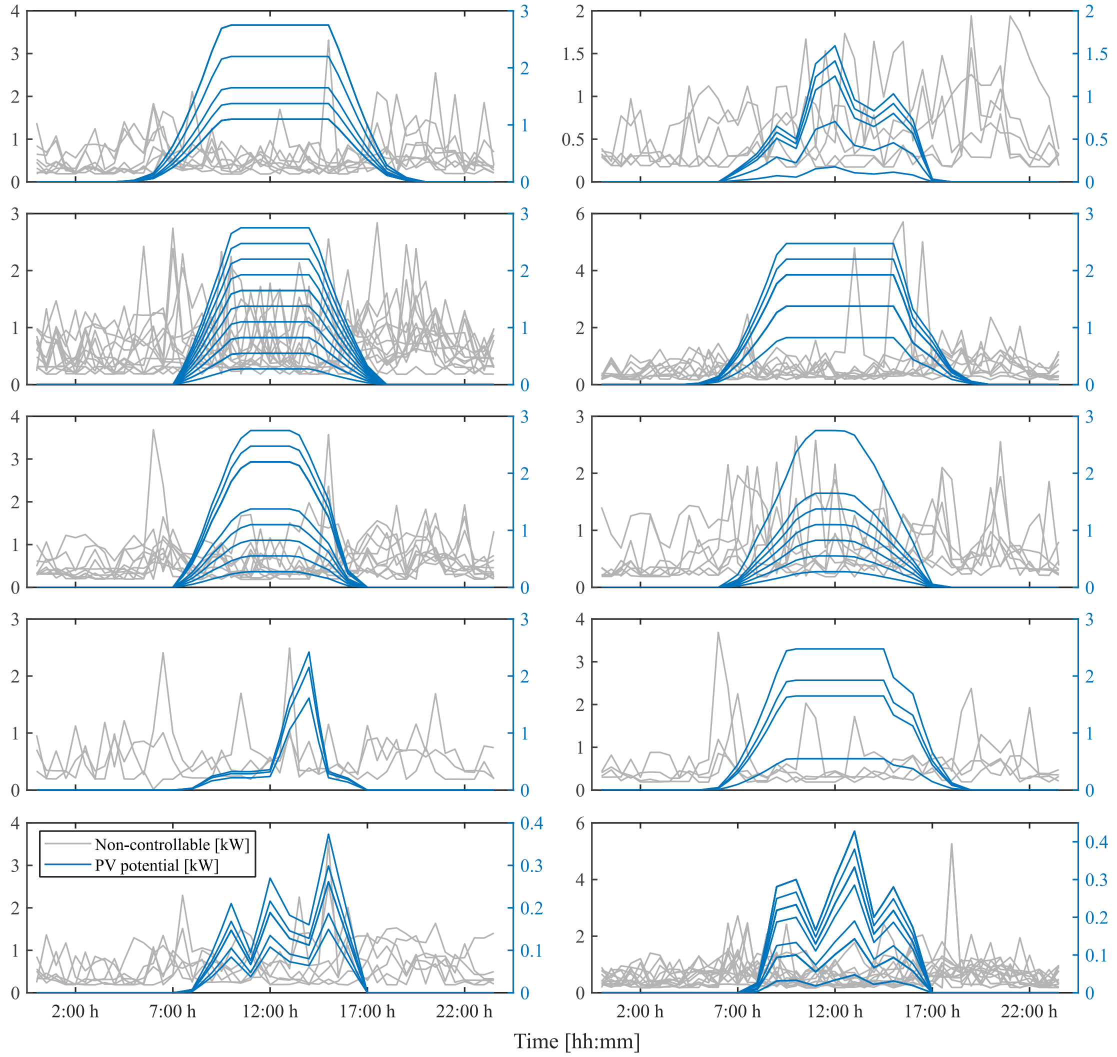

Fig. 9 - Expected non-controllable demand and PV generation in ECs starting from EC #1 at top far left corner and ending with EC #10 at bottom far right corner

Table 1 - A summary of ECs data

# EC	No. of prosumers	Total PV capacity	Total storage capacity	Total EV capacity	Total HVAC power installed	No. of CAs
1	8	12.75 kWp	24 kWh	142 kWh	16.5 kW	19
2	5	5.25 kWp	13 kWh	61 kWh	11 kW	17
3	13	16.5 kWp	37 kWh	222 kWh	26.5 kW	39
4	9	14 kWp	28 kWh	166 kWh	17.5 kW	33
5	10	14.5 kWp	28 kWh	168 kWh	20 kW	26
6	7	7.75 kWp	11.5 kWh	108 kWh	13.5 kW	17
7	3	6.5 kWp	12.5 kWh	59 kWh	4.5 kW	12
8	4	6 kWp	5.5 kWh	55 kWh	8 kW	16
9	6	8 kWp	17 kWh	85 kWh	12.5 kW	17
10	15	16.5 kWp	39 kWh	258 kWh	30.5 kW	40

6.2 - Results: deterministic case

To validate the proposed mathematical model, we analyse the deterministic case, for which uncertainties are neglected. Fig. 10 shows the scheduling result for the distributed assets (storage systems and renewable generators). As seen, peak generation occurs in the morning when the wind generation reaches its maximum and the PV generation of plant #2 rapidly increases. This high renewable generation enables selling surplus energy to the utility grid and thus obtaining a monetary revenue. During night, the low demand allows to sell the surplus wind generation to the utility grid. This process is complemented by the storage systems, which allow to increment the exportable energy. During midday, the renewable generation is still high regardless of the reduced wind generation since PV plant #1 has reached its maximum generation capacity. During these periods, the DN profusely operates the distributed storage assets to sell as much energy as possible. At about 17:00 h, the purchasing price reaches its maximum; in this situation, the storage systems are mostly discharged to fully cover the local demand and thus reduce the energy imported from the grid. At this hour, the selling price is also high. However, the local generation is not sufficient to produce surplus energy that could eventually be exported. During the night, the DN acts as a consumer primarily since renewable generation falls to its minimum. Thus, much energy must be imported to cover the demand and charge the batteries to recover their SOC.

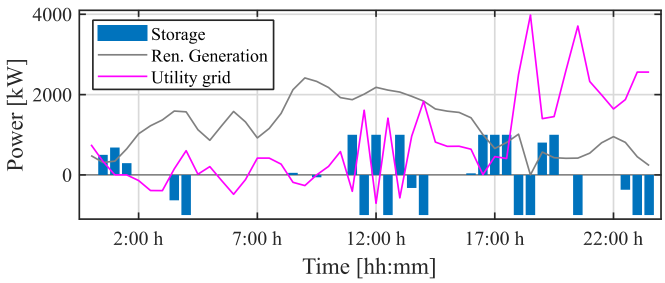

Fig. 10 - Scheduling result for the distributed assets under deterministic conditions.

Fig. 11 is analog to Fig. 10 but particularizing for EC #1 (for simplicity, only one EC is analysed, being possible to yield the same conclusions for the other communities). At noon, BESs and EVs are first discharged to increment the exportable energy. Posteriorly, EVs are charged, and most CAs are scheduled, coinciding with the beginning of their time windows. As such, the peak demand is observed at about 4:00 h, which occurs when the purchasing price is low. In the morning, when the PV generation increases, demand attributable to CAs is still high, and non-controllable demand grows. Increasing PV generation together with the completed duty cycles allow to progressively reduce the imported energy to zero at about 9:00 h, thus turning the community into a net generator at about 12:00 h, when the PV generation achieves its maximum. Similar to the DN, BESs are profusely scheduled during the evening to either increase the exportable power or reduce the imported energy. These processes are focused on improving the economy of the EC since, during these periods, both selling and purchasing prices achieve their maximum values. When the PV generation approaches zero at night, the second peak demand is observed, mainly because many CAs must be scheduled during the night, due to their predefined time windows.

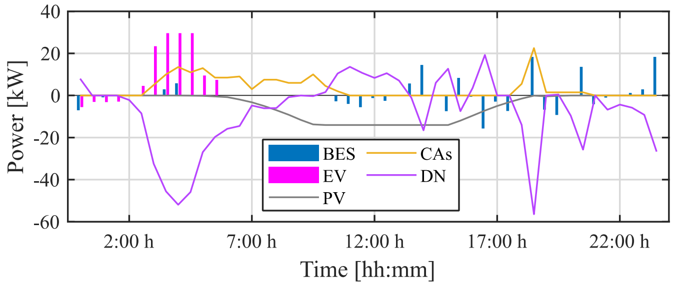

Fig. 11 - Scheduling result for EC #1 under deterministic conditions. In this figure, negative values indicate 'to-the-EC' flow direction

6.3 - Impact of uncertainties

In the developed framework, uncertainties are incorporated via interval modelling and iterative procedure. This methodology allows to adopt two different strategies, namely optimistic and pessimistic, depending on the assumed deviation of uncertainties. Thus, if the operator assumes a pessimistic perspective, the results obtained will be risk-averse. If a negative impact of uncertainties is assumed, the results will be risk-seeker otherwise. It is observed in Fig. 12, where the actual wind and PV generation are compared under deterministic conditions and optimistic and pessimistic strategies ($\xi = 1$), that this adoption has a notable impact on the results,. As seen in this figure, the developed optimization tool assumes more favourable or unfavourable profiles depending if the operator adopts an optimistic or pessimistic scheduling strategy. Thus, less renewable generation is expected in case of assuming a pessimistic perspective. Actually, total renewable generation is reduced by 19% under pessimistic circumstances, while this parameter increases by 16% when an optimistic point of view is adopted.

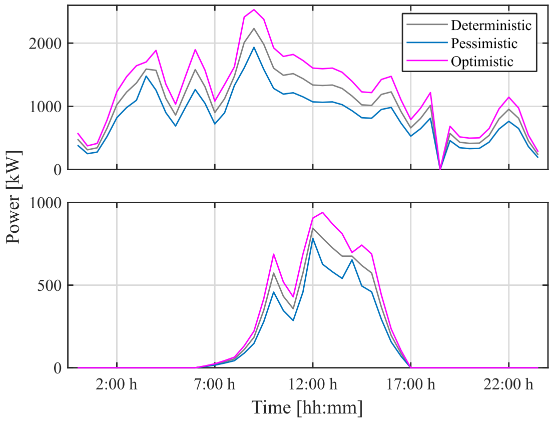

Fig. 12 - Actual wind (top) and PV (bottom) generation under deterministic, pessimistic and optimistic conditions ($\xi = 1$)

The uncertainties also notably impact on utility energy prices, under which the DN exchanges energy with the utility grid. In this regard, Fig. 13 compares the average purchasing and selling prices for different cases. As observed, purchasing prices are considered higher when adopting a pessimistic strategy, while the opposite is assumed under optimistic conditions. In contrast, selling energy prices increase under optimistic conditions and decrease when a pessimistic strategy is assumed. The variation of energy prices with respect to expected profiles leads to a more favourable or unfavourable cost-revenue balance depending on the operational strategy adopted. Thus, the total purchasing cost notably increases in the pessimistic case. It is noteworthy that this parameter scarcely grows in the optimistic case. However, extra monetary expenditures are compensated by a notable revenue increment by selling energy, while this parameter falls to zero in the pessimistic case. This result is due to the fact that the DN imports more energy in both the optimistic and pessimistic cases, as seen in Fig. 14. However, this amount of energy can be more efficiently managed in the former case. Indeed, in the optimistic case, energy can be imported cheaper and sold at a higher cost, for which storage systems play a vital role.

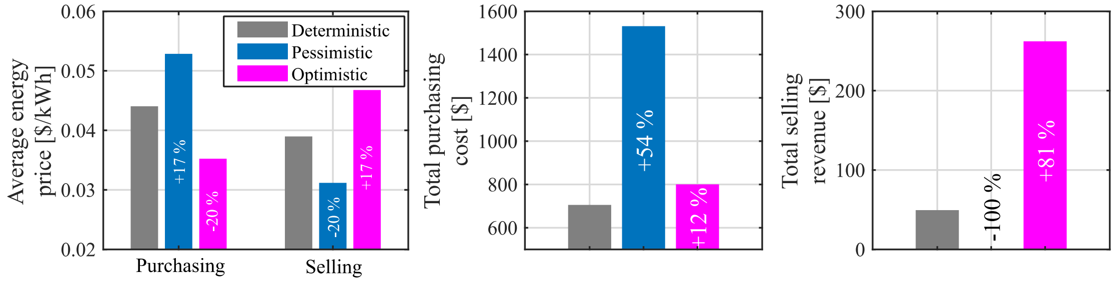

Fig. 13 - Average purchasing and selling prices (left), total purchasing cost (center), and total selling revenue (right) for the DN under deterministic, pessimistic, and optimistic conditions ($\xi = 1$). Inside the bars, the variation with respect to the deterministic case is shown

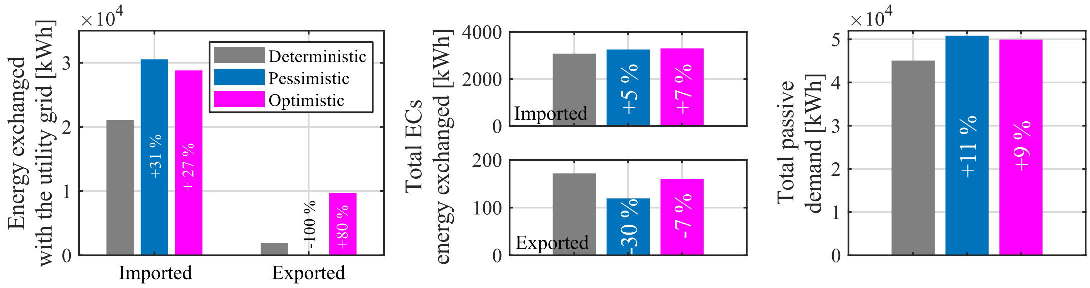

Fig. 14 - Total energy exchanged with the utility grid (left), with ECs (center) and total passive consumers demand (right) under deterministic, pessimistic, and optimistic conditions ($\xi = 1$). Inside the bars, the variation with respect to the deterministic case is shown

It is remarkable that local demand is higher when uncertainties are considered. In the pessimistic case, this circumstance forces to purchase much energy from the utility grid at a high price. In contrast, when adopting an optimistic perspective, this demand can be supplied from either cheap energy from the utility but also from renewable generators. This increasing demand, together with the assumed high renewable generation, bring additional income to the DSO, thus improving the monetary balance. Finally, exported energy from ECs decrease in both the pessimistic and optimistic case. In the former case is due to the negative impact of uncertainties that reduce the exportable energy from ECs. Whereas, in the latter case, the DN does not need to acquire much energy from the communities since the renewable generation is high. In this context, the developed methodology prioritizes acquiring energy from renewable generators since exported energy from ECs may eventually be expensive and limited.

The developed methodology has the advantage of being adaptable by adjusting the value of the uncertain level (i.e., ξ). This parameter sets the degree in which the confidence intervals are considered, in the way that the higher value of ξ, the more uncertain-oriented the scheduling result is. Fig. 15 shows that ξ has an evident impact on the monetary balance for the DSO. As seen, total incomes grow with the uncertain level in the optimistic case, expecting to be incremented by 22 % at extreme values. On the other hand, the monetary revenues are progressively reduced as more pessimistic conditions are assumed. In particular, total profit falls by 28 % for $\xi = 1$. This monetary reduction is known as the cost of robustness [61] since it represents the monetary loss that the operator must assume to obtain a risk-averse result.

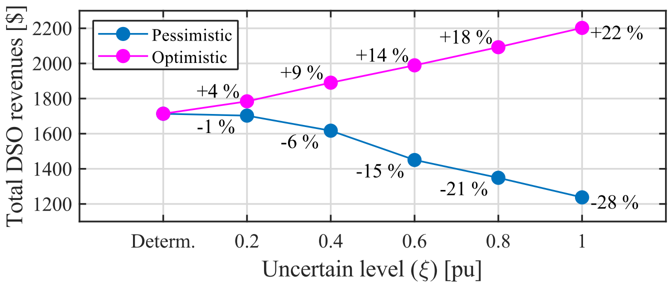

Fig. 15 - Total DSO revenues for various values of ξ

6.4 - Profit analysis

The developed methodology incorporates a sub-routine to determine the DSO profit to maximize collective welfare (see Section 5). This section analyses how uncertainties affect the DSO profit. Fig. 16 reports the DSO profit for different values of the uncertain level. In the optimistic case, the optimal profit value seems independent of ξ, keeping relatively constant about 5 % in the range $\xi \in [0, 1]$. However, as seen in Fig. 15, the total monetary revenues grow with the value of the uncertain parameter. The explanation of this result is illustrated in Fig. 17, where the monetary balances of the different agents connected to the DN, i.e., large passive consumers and ECs, are presented. As seen, monetary expenditures of all the consumers connected to the DN grow, thus incrementing the incomes for the DSO. It is worth noting that ECs revenues by exporting energy also increase with the uncertain level. However, payments transferred from the DSO by this service are not high and eventually avoid importing energy from the community. In such circumstances, the DSO profit does not necessarily increase with the uncertain level since the favourable value of uncertainties (higher renewable generation and demand together with lower prices) favors the increment of monetary revenues without incrementing the profit, which may provoke undesirable effects (e.g., reduction of exportable energy from ECs).

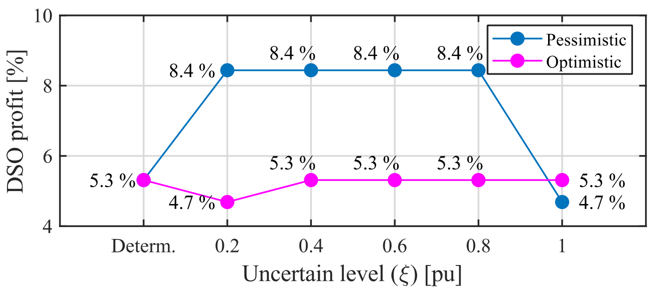

Fig. 16 - Total DSO revenues for various values of ξ

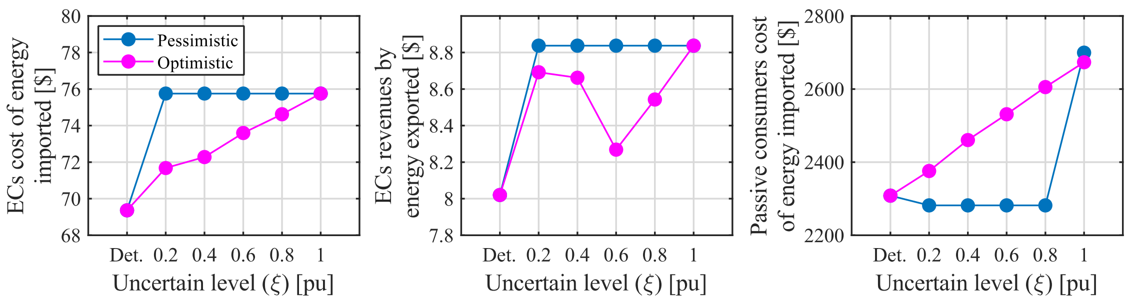

Fig. 17 - Monetary balances for ECs and passive consumers for various values of ξ

On the other hand, the profit grows to 8.4 % under pessimistic conditions, keeping constant in the range $\xi \in [0, 0.8]$. In this case, the DSO needs to increase his own profit in order to maintain his level of income, which inevitably decreases because of the negative impact of uncertainties (see Fig. 15). When the effect of uncertainties becomes notable, expenditures of ECs notably increase together with the incomes from exporting energy. This is because, in such circumstances, the ECs sell energy at higher prices and import power from the DN at a higher cost. Despite that, the DSO still needs to import energy from ECs to compensate for the lower renewable generation in the network. When $\xi = 1$, the DSO profit can be reduced to 4.7 %. This is due to a notable increment in passive demand that increases the monetary incomes for the DSO. In this context, the DSO can afford to reduce his profit to maintain social welfare.

7 - Conclusions and future works

A novel bi-level scheduling strategy for active DNs has been developed. The new proposal envisages a bi-level framework by which operators schedule ECs at the lower level while DSO directly manages distributed assets at the upper level. To cope with uncertainties in demand, generation, and energy prices, a novel MILP interval-based formulation has been proposed, which effectively handles with uncertain parameters without degrading the computational efficiency of the optimization framework. An effective yet simple sub-module has been designed to determine the distribution prices based on an original Stackelberg-bisection procedure.

The case study on the IEEE 33-bus network has been analysed, incorporating 10 ECs, 6 passive consumers, and a variety of distributed renewable generators and storage assets. The results validated the model by analysing the deterministic case, yielding interpretable results. Secondly, the impact of uncertainties has been studied, concluding that the level of robustness directly affects renewable generation and demand, allowing to adopt pessimistic or optimistic strategies. In this context, uncertainty-aware results can be obtained but at the expense of reducing the DSO revenues by 28 % under pessimistic conditions, while risk-seeker strategies would enable increment of the monetary incomes by 22 %. Finally, a profit analysis has been presented, demonstrating that the profit determination in DNs encompassing ECs is a complex task, which must consider the individual consumption and the exportable capacity of communities.

Future work is to investigate active DNs in the presence of ECs by incorporating more advanced demand response strategies.

Appendix A - Decision variables

The vectors of decision variables mentioned throughout the paper are fully defined in (A1)-(A5).

$$\boldsymbol{x}_c^{EC} = \left\{ \begin{matrix} p_{i|t}^{DN,k};\ p_{i|t}^{PV};\ p_{i|t}^{BES,l}; \\ p_{i|t}^{EV,l}; p_{i\to j|t}^{P2P}; p_{i|t}^{HVAC,m}; \\ \varepsilon_{i|t}^{BES}; \varepsilon_{i|t}^{EV}; T_{i|t}^{Air,in} \end{matrix} \right\}; \begin{matrix} \forall i,j \in \boldsymbol{\mathcal{P}}_c \wedge c \in \boldsymbol{\mathcal{EC}} \wedge t \in \boldsymbol{\mathcal{T}} \wedge k \in \{buy; sell\} \\ \wedge\, l \in \{ch; dch\} \wedge m \in \{hot; cool\} \end{matrix} \quad \text{(A1)}$$

$$\boldsymbol{u}_c^{EC} = \left\{ \begin{matrix} u_{i|t}^{DN,k}; u_{i|t}^{a}; u_{i|t}^{BES,l}; u_{i|t}^{EV,l}; \\ u_{i|t}^{HVAC,m}; on_{i|t}^{aa}; off_{i|t}^{aa} \end{matrix} \right\}; \begin{matrix} \forall i \in \boldsymbol{\mathcal{P}}_c \wedge c \in \boldsymbol{\mathcal{EC}} \wedge t \in \boldsymbol{\mathcal{T}} \wedge k \in \{buy; sell\} \\ \wedge\, a \in \left\{\boldsymbol{\mathcal{A}}_i^{I} \cup \boldsymbol{\mathcal{A}}_i^{NI}\right\} \wedge l \in \{ch; dch\} \\ \wedge\, m \in \{hot; cool\} \wedge aa \in \boldsymbol{\mathcal{A}}_i^{NI} \end{matrix} \quad \text{(A2)}$$

$$\boldsymbol{x}^{DN} = \left\{ \begin{matrix} p_t^{UG,k}; p_{g|t}; p_{c|t}^{DN,k}; \\ p_{s|t}^{BES,l}; P_{b|t}; V_{b|t}; \varepsilon_{s|t}^{BES} \end{matrix} \right\}; \begin{matrix} \forall t \in \boldsymbol{\mathcal{T}} \wedge k \in \{buy; sell\} \\ \wedge\, g \in \boldsymbol{\mathcal{G}} \wedge c \in \boldsymbol{\mathcal{EC}} \wedge s \in \boldsymbol{\mathcal{S}} \\ \wedge\, l \in \{ch; dch\} \wedge b \in \boldsymbol{\mathcal{B}} < |\boldsymbol{\mathcal{B}}| \end{matrix} \quad \text{(A3)}$$

$$\boldsymbol{u}^{DN} = \left\{u_t^{UG,k}; u_{s|t}^{BES,l}\right\}; \forall t \in \boldsymbol{\mathcal{T}} \wedge k \in \{buy; sell\} \wedge s \in \boldsymbol{\mathcal{S}} \wedge l \in \{ch; dch\} \quad \text{(A4)}$$

$$\boldsymbol{\Psi} = \left\{ \begin{matrix} z_t^{UG,k}; \varphi_{t|i}^{UG,k}; \\ \delta\tilde{\pi}_{t|i}^{UG,l}; \delta p_{t|i}^{UG,l}; \delta z_t \end{matrix} \right\};\ \forall t \in \boldsymbol{\mathcal{T}} \wedge k \in \{buy; sell\} \wedge i \in \{1,2,\dots,n\} \quad \text{(A5)}$$

Appendix B - Proofs of existence and uniqueness for the Stackelber game described in Section 5

To formally describe the Stackelberg game framework defined in Section 5, we need to prove its existence and uniqueness [51], whose proofs are detailed below.

<u>Proof of existence</u>

When the following conditions are met, there exists a Stackelber equilibrium solution.

1. The leader's objective function is the non-empty continuous function of all game strategies.
2. The objective function of each follower is a non-empty continuous function of all game strategies.
3. The objective function of each follower is the quasi-convex function of its own strategy.

Proof of 1

The objective function of the DSO (21) can be rewritten as a function of the profit, as follows:

$$F^{DSO} = \Delta t \cdot \sum_{t\in\mathcal{T}} \left\{ \pi_t^{UG,sell} \cdot p_t^{UG,sell} - \pi_t^{UG,buy} \cdot p_t^{UG,buy} + \sum_{c\in\mathcal{EC}} \left\{ (1+\lambda) \cdot \pi_t^{UG,buy} \cdot p_{c|t}^{DN,buy} - (1-\lambda) \cdot \pi_t^{UG,sell} \cdot p_{c|t}^{DN,sell} \right\} + \sum_{c\in\mathcal{C}} \left\{ (1+\lambda) \cdot \pi_t^{UG,buy} \cdot p_{c|t}^{DN,buy} \right\} \right\} \quad \text{(B1)}$$

This agent partakes in the game by adjusting his own profit λ. Thereby, for a given followers' strategy, the first partial derivative of (B1) is

$$\frac{\partial F^{DSO}}{\partial \lambda} = \Delta t \cdot \sum_{t\in\mathcal{T}} \left\{ \sum_{c\in\mathcal{EC}} \left\{ \pi_t^{UG,sell} \cdot p_{c|t}^{DN,sell} + \pi_t^{UG,buy} \cdot p_{c|t}^{DN,buy} \right\} + \sum_{c\in\mathcal{C}} \left\{ \pi_t^{UG,buy} \cdot p_{c|t}^{DN,buy} \right\} \right\} \quad \text{(B2)}$$

From (B2) it is evident that (B1) is a continuously increasing function of λ, since $p_{c|t}^{EC,sell}$ and $p_{c|t}^{EC,buy}$ are greater than zero $\forall c \in \{\mathcal{EC} \cup \mathcal{C}\} \wedge t \in t \in \mathcal{T}$, and negative prices are not allowed. On the other hand, the strategy set of DSO is non-empty given these conditions [62].

Proof of 2

The objective function for ECs can be rewritten as a function of the DSO's profit, as follows:

$$F_c^{EC} = \Delta t \cdot \sum_{t\in\mathcal{T}} \left\{ (1+\lambda) \cdot \pi_t^{UG,buy} \cdot p_{c|t}^{DN,buy} - (1-\lambda) \cdot \pi_t^{UG,sell} \cdot p_{c|t}^{DN,sell} \right\}; \forall c \in \mathcal{EC} \quad \text{(B3)}$$

ECs participate by adjusting their own import/export profile as response to the prices fixed by DSO. Therefore, the first partial derivatives of (B3) with respect ECs' strategy is

$$\frac{\partial F_c^{EC}}{\partial p_{c|t}^{buy}} = (1+\lambda) \cdot \pi_t^{UG,buy}, \ \frac{\partial F_c^{EC}}{\partial p_{c|t}^{sell}} = (\lambda - 1) \cdot \pi_t^{UG,sell}; \ \forall c \in \mathcal{EC} \quad \text{(B4)}$$

From (B4) it is clear that (B3) is a continuous function of the ECs' strategy. In addition, since negative prices and profit are not allowed, the strategy set of ECs is non-empty [62].

Likewise, for the passive consumers one has

$$F_c^{C} = \Delta t \cdot \sum_{t\in\mathcal{T}} \left\{ (1+\lambda) \cdot \pi_t^{UG,buy} \cdot p_{c|t}^{DN,buy} \right\}; \forall c \in \mathcal{C} \quad \text{(B5)}$$

Whose continuous and non-emptiness proofs are trivial by observing (B4).

Proof of 3

The second partial derivatives of (B3) and (B5) with respect their strategies yield zero, which indicates that both functions are concave [62].

<u>Proof of uniqueness</u>

When the game model satisfies the following conditions, there is a unique Stackelberg equilibrium solution.

a. When the leader's strategy is given, all the followers have unique optimal solutions.
b. When the follower's strategy is given, the leader has a unique optimal solution.

Proof of a

By observing (B4) and assuming $\lambda < 1$, it is clear that (B3) is a continuously increasing function of $p_{c|t}^{buy}$ and decreasing of $p_{c|t}^{sell}$ $\forall c \in \mathcal{EC} \wedge t \in t \in \mathcal{T}$. On the other hand, the second partial derivatives of (B3) and (B5) yield zero, which indicates concavity. These two results demonstrate that (B3) and (B5) have a unique optimal solution within allowable ranges of λ.

Proof of b

This proof is trivial by observing (B2), since (B1) is a continuously decreasing function of λ and, in consequence, it has a unique solution.

Acknowledgments

The icons used in this paper were obtained from www.svgrepo.com.

References

[1] Department of Energy. Reducing Electricity Use and Costs. Online, available at: https://www.energy.gov/energysaver/reducing-electricity-use-and-costs, (accessed on Aug. 3, 2022).

[2] European Commission. Save Gas for a Safe Winter: Commission proposes gas demand reduction plan to prepare EU for supply cuts. Press release; Jul. 20, 2022. Online, available at: https://ec.europa.eu/commission/presscorner/detail/en/IP_22_4608, (accessed on Aug. 3, 2022).

[3] International Energy Agency. Energy saving actions by EU citizens could save enough oil to fill 120 super tankers and enough natural gas to heat 20 million homes. Press release; Apr. 21, 2022. Online, available at: https://www.iea.org/news/energy-saving-actions-by-eu-citizens-could-save-enough-oil-to-fill-120-super-tankers-and-enough-natural-gas-to-heat-20-million-homes, (accessed on Aug. 3, 2022).

[4] S. Rajamand. Probabilistic Power Distribution Considering Uncertainty in Load and Distributed Generators Using Cumulant and Truncated Versatile Distribution. *Sustainable Energy, Grids and Networks* 2022; 30: 100608. https://doi.org/10.1016/j.segan.2022.100608.

[5] M. Tan, Y. Zhou, L. Wang, Y. Su, B. Duan, R. Wang. Fair-efficient energy trading for microgrid cluster in an active distribution network. *Sustainable Energy, Grids and Networks* 2021; 26: 100453. https://doi.org/10.1016/j.segan.2021.100453.

[6] M. Mousavi, M. Wu. A DSO Framework for Market Participation of DER Aggregators in Unbalanced Distribution Networks. *IEEE Transactions on Power Systems* 2022; 37(3): 2247-58. https://doi.org/10.1109/TPWRS.2021.3117571.

[7] H. Ren, Z. Ma, A.M.L. Fong, Y. Sun. Optimal deployment of distributed rooftop photovoltaic systems and batteries for achieving net-zero energy of electric bus transportation in high-density cities. *Applied Energy* 2022; 319: 119274. https://doi.org/10.1016/j.apenergy.2022.119274.

[8] M.L. Lode, G. te Boveldt, T. Coosemans, L.R. Camargo. A transition perspective on Energy Communities: A systematic literature review and research agenda. *Renewable & Sustainable Energy Reviews* 2022; 163: 112479. https://doi.org/10.1016/j.rser.2022.112479.

[9] J.M. Morales, S. Pineda, Y. Dvorkin. Learning the Price Response of Active Distribution Networks for TSO-DSO Coordination. *IEEE Transactions on Power Systems* 2022; 37(4): 2858-68. https://doi.org/10.1109/TPWRS.2021.3127343.

[10] European Parliament and Council. Directive (EU) 2019/944 of the European Parliament and of the Council of 5 Jun. 2019 on common rules for the internal market for electricity and amending directive 2012/27/EU. *Official Journal European Union* 2019; 158: 125-199.

[11] A. Fazeli, E. Christopher, C.M. Johnson, M. Gillott, M. Sumner. Investigating the effects of dynamic demand side management within intelligent Smart Energy communities of future decentralized power system. In *2011 2nd IEEE PES International Conference and Exhibition on Innovative Smart Grid Technologies*, Manchester, UK, 2011: 1-8. https://doi.org/10.1109/ISGTEurope.2011.6162619.

[12] J. Burch, J. Woods, E. Kozubal, A. Boranian. Zero Energy Communities with Central Solar Plants using Liquid Desiccants and Local Storage. *Energy Procedia* 2012; 30: 55-64. https://doi.org/10.1016/j.egypro.2012.11.008.

[13] B.P. Koirala, E. Koliou, J. Friege, R.A. Hakvoort, P.M. Herder. Energetic communities for community energy: A review of key issues and trends shaping integrated community energy systems. *Renewable and Sustainable Energy Reviews* 2016; 56: 722-44. https://doi.org/10.1016/j.rser.2015.11.080.

[14] M.H. Bashi, et al. A review and mapping exercise of energy community regulatory challenges in European member states based on a survey of collective energy actors. *Renewable and Sustainable Energy Reviews* 2023; 172: 113055. https://doi.org/10.1016/j.rser.2022.113055.

[15] A. Uihlein, A. Caramizaru. *Energy communities: an overview of energy and social innovation*. European Commission, Joint Research Centre, 2020. https://data.europa.eu/doi/10.2760/180576.

[16] A. Eshan, Q. Yang. State-of-the-art techniques for modelling of uncertainties in active distribution network planning: A review. *Applied Energy* 2019; 239: 1509-23. https://doi.org/10.1016/j.apenergy.2019.01.211.

[17] X. Liu, Z. Yan, J. Wu. Optimal coordinated operation of a multi-energy community considering interactions between energy storage and conversion devices. *Applied Energy* 2019; 248: 256-73. https://doi.org/10.1016/j.apenergy.2019.04.106.

[18] S. Lilla, C. Orozco, A. Borghetti, F. Napolitano, F. Tossani. Day-ahead scheduling of a local energy community: An alternating direction method of multipliers approach. *IEEE Transactions on Power Systems* 2020; 35(2): 1132-42. https://doi.org/10.1109/TPWRS.2019.2944541.

[19] H.-C. Jo, G. Byeon, J.-Y. Kim, S.-K. Kim. Optimal scheduling for a zero net energy community microgrid with customer-owned energy storage systems. *IEEE Transactions on Power Systems* 2021; 36(3): 2273-80. https://doi.org/10.1109/TPWRS.2020.3036077.

[20] C. Feng, F. Wen, S. You, Z. Li, F. Shahnia, M. Shahidehpour. Coalitional Game-Based Transactive Energy Management in Local Energy Communities. *IEEE Transactions on Power Systems* 2020; 35(3): 1729-40. https://doi.org/10.1109/TPWRS.2019.2957537.

[21] A. Cosic, M. Stadler, M. Mansoor, M. Zellinger. Mixed-integer linear programming based optimization strategies for renewable energy communities. *Energy* 2021; 237: 121559. https://doi.org/10.1016/j.energy.2021.121559.

[22] H. Nagpal, I.-I. Avramidis, F. Capitanescu, A.G. Madureira. Local Energy Communities in Service of Sustainability and Grid Flexibility Provision: Hierarchical Management of Shared Energy Storage. *IEEE Transactions on Sustainable Energy* 2022; 13(3): 1523-35. https://doi.org/10.1109/TSTE.2022.3157193.

[23] Z. Liu et al. Co-optimization of a novel distributed energy system integrated with hybrid energy storage in different nearly zero energy community scenarios. *Energy* 2022; 247: 123553. https://doi.org/10.1016/j.energy.2022.123553.

[24] A.D. Mustika, R. Rigo-Mariani, V. Debusschere, A. Pachurka. A two-stage management strategy for the optimal operation and billing in an energy community with collective self-consumption. *Applied Energy* 2022; 310: 118484. https://doi.org/10.1016/j.apenergy.2021.118484.

[25] B. Yan, M. Di Somma, G. Graditi, P.B. Luh. Markovian-based stochastic operation optimization of multiple distributed energy systems with renewables in a local energy community. *Electric Power Systems Research* 2020; 186: 106364. https://doi.org/10.1016/j.epsr.2020.106364.

[26] N. Vespermann, T. Hamacher, J. Kazempour. Risk Trading in Energy Communities. *IEEE Transactions on Smart Grid* 2021; 12(2): 1249-63. https://doi.org/10.1109/TSG.2020.3030319.

[27] C. Orozco, A. Borghetti, B. De Schutter, F. Napolitano, G. Pulazza, F. Tossani. Intra-day scheduling of a local energy community coordinated with day-ahead multistage decisions. *Sustainable Energy, Grids & Networks* 2022; 29: 100573. https://doi.org/10.1016/j.segan.2021.100573.

[28] S. Sarfarazi, S. Mohammadi, D. Khastieva, M.R. Hesamzadeh, V. Bertsch, D. Bunn. An optimal real-time pricing strategy for aggregating distributed generation and battery storage systems in energy communities: A stochastic bilevel optimization approach. *International Journal of Electrical Power & Energy Systems* 2023; 147: 108770. https://doi.org/10.1016/j.ijepes.2022.108770.

[29] M. Tostado-Véliz, S. Kamel, H.M. Hasanien, R.A. Turky, F. Jurado. Optimal energy management of cooperative energy communities considering flexible demand, storage and vehicle-to-grid under uncertainties. *Sustainable Cities & Society* 2022; 84: 104019. https://doi.org/10.1016/j.scs.2022.104019.

[30] M. Tostado-Véliz, S.A. Mansouri, A. Rezaee-Jordehi, D. Icaza-Alvarez, F. Jurado. Information Gap Decision Theory-based day-ahead scheduling of energy communities with collective hydrogen chain. *International Journal of Hydrogen energy* 2023; 48(20): 7154-69. https://doi.org/10.1016/j.ijhydene.2022.11.183.

[31] B.V. Rao et al. Optimal capacity management applied to a low voltage distribution grid in a local peer-to-peer energy community. *International Journal of Electrical Power & Energy Systems* 2022; 134: 107355. https://doi.org/10.1016/j.ijepes.2021.107355.

[32] D.F. Botelho, L.W. de Oliveira, B.H. Dias, T.A. Soares, C.A. Moraes. Integrated prosumers–DSO approach applied in peer-to-peer energy and reserve tradings considering network constraints. *Applied Energy* 2022; 317: 119125. https://doi.org/10.1016/j.apenergy.2022.119125.

[33] B. Wang, C. Zhang, Z.Y. Dong. Interval Optimization Based Coordination of Demand Response and Battery Energy Storage System Considering SOC Management in a Microgrid. *IEEE Transactions on Sustainable Energy* 2020; 11(4): 2922-31. https://doi.org/10.1109/TSTE.2020.2982205.

[34] G. Iazzolino, N. Sorrentino, D. Menniti, A. Pinnarelli, M. De Carolis, L. Mendicino. Energy communities and key features emerged from business models review. *Energy Policy* 2022; 165: 112929. https://doi.org/10.1016/j.enpol.2022.112929.

[35] A. Dong, T. Baroche, R.L.G. Latimier, H.B. Ahmed. Convergence analysis of an asynchronous peer-to-peer market with communication delays. *Sustainable Energy, Grids and Networks* 2021; 26: 100475. https://doi.org/10.1016/j.segan.2021.100475.

[36] OMIE. Day-ahead hourly price. Online, available at: https://www.omie.es/en/market-results/daily/daily-market/daily-hourly-price, (accessed on Aug. 4, 2022).

[37] I. Alsaidan, A. Khodaei, W. Gao. A Comprehensive Battery Energy Storage Optimal Sizing Model for Microgrid Applications. *IEEE Transactions on Power Systems* 2018; 33(4): 3968-80. https://doi.org/10.1109/TPWRS.2017.2769639.

[38] M. Tostado-Véliz, S. Kamel, F. Aymen, A.R. Jordehi, F. Jurado. A Stochastic-IGDT model for energy management in isolated microgrids considering failures and demand response. *Applied Energy* 2022; 317: 119162. https://doi.org/10.1016/j.apenergy.2022.119162.

[39] M. Tostado-Véliz, R.S. León-Japa, F. Jurado. Optimal electrification of off-grid smart homes considering flexible demand and vehicle-to-home capabilities. *Applied Energy* 2021; 298: 117184. https://doi.org/10.1016/j.apenergy.2021.117184.

[40] M. Tostado-Véliz, S. Gurung, F. Jurado. Efficient solution of many-objective Home Energy Management systems. *International Journal of Electrical Power & Energy Systems* 2022; 136: 107666. https://doi.org/10.1016/j.ijepes.2021.107666.

[41] Z. Wang, B. Chen, J. Wang, M.M. Begovic, C. Chen. Coordinated energy management of networked microgrids in distribution systems. *IEEE Transactions on Smart Grid* 2015; 6(1): 45-53. https://doi.org/10.1109/TSG.2014.2329846.

[42] K. Turitsyn, P. Šulc, S. Backhaus, M. Chertkov. Distributed control of reactive power flow in a radial distribution circuit with high photovoltaic penetration. *IEEE PES General Meeting, 2010*; Minneapolis, MN, U.S.: 1-6. https://doi.org/10.1109/PES.2010.5589663.

[43] A.R. Silva, H.M.I. Pousinho, A. Estanqueiro. A multistage stochastic approach for the optimal bidding of variable renewable energy in the day-ahead, intraday and balancing markets. *Energy* 2022; 258: 124856. https://doi.org/10.1016/j.energy.2022.124856.
[44] B. Park et al. Optimal Demand Response Incorporating Distribution LMP With PV Generation Uncertainty. *IEEE Transactions on Power Systems* 2022; 37(2): 982-95. https://doi.org/10.1109/TPWRS.2021.3107671.
[45] R. Nourollahi, P. Salyani K. Zare, R. Razzaghi. A two-stage hybrid robust-stochastic day-ahead scheduling of transactive microgrids considering the possibility of main grid disconnection. *International Journal of Electrical Power & Energy Systems* 2022; 136: 107701. https://doi.org/10.1016/j.ijepes.2021.107701.
[46] A. Mansour-Saatloo et al. Multi-objective IGDT-based scheduling of low-carbon multi-energy microgrids integrated with hydrogen refueling stations and electric vehicle parking lots. *Sustainable Cities & Society* 2021; 74: 103197. https://doi.org/10.1016/j.scs.2021.103197.
[47] C. Rooks et al. Robust hierarchical dispatch for residential distribution network management considering home thermal flexibility and model predictive control. *IET Generation, Transmission & Distribution* 2021; 15(18): 2567-81. https://doi.org/10.1049/gtd2.12199.
[48] M. Tostado-Véliz, S. Kamel, H.M. Hasanien, R.A. Turky, F. Jurado. A mixed-integer-linear-logical programming interval-based model for optimal scheduling of isolated microgrids with green hydrogen-based storage considering demand response. *Journal of Energy Storage* 2022; 48: 104028. https://doi.org/10.1016/j.est.2022.104028.
[49] C.E. Gounaris, R. Misener, C.A. Floudas. Computational comparison of piecewise-linear relaxations for pooling problems. *Industrial & Engineering Chemical Research* 2009; 48(12): 5742–66. https://doi.org/10.1021/ie8016048.
[50] Y. Li, C. Wang, G. Li, J. Wang, D. Zhao, C. Chen. Improving operational flexibility of integrated energy system with uncertain renewable generations considering thermal inertia of buildings. *Energy Conversion & Management* 2020; 207: 112526. https://doi.org/10.1016/j.enconman.2020.112526.
[51] Y. Li, B. Wang, Z. Yang, J. Li, C. Chen. Hierarchical stochastic scheduling of multi-community integrated energy systems in uncertain environments via Stackelberg game. *Applied Energy* 2022; 308: 118392. https://doi.org/10.1016/j.apenergy.2021.118392.
[52] C. Gómez-Quiles, A. Gómez-Expósito, W. Vargas. Computation of Maximum Loading Points via the Factored Load Flow. *IEEE Transactions on Power Systems* 2016; 31(5): 4128-34. https://doi.org/10.1109/TPWRS.2015.2505185.
[53] A.J. Conejo, M. Carrión, J.M. Morales. *Decision Making Under Uncertainty in Electricity Markets*. New York, NY: Springer, 2010.
[54] R.D. Zimmerman, C.E. Murillo-Sánchez, R.J. Thomas. MATPOWER: Steady-State Operations, Planning, and Analysis Tools for Power Systems Research and Education. *IEEE Transactions on Power Systems* 2011; 26(1): 12-9. https://doi.org/10.1109/TPWRS.2010.2051168.
[55] National Centers for Environmental Information. Land base datasets. Online, available at: https://www.ncei.noaa.gov/products/land-based-station, (accessed on Sep. 15, 2022).
[56] Red Eléctrica de España. Canary electricity demand in real-time. Online, available at: https://www.ree.es/en/activities/canary-islands-electricity-system/canary-electricity-demand-in-real-time, (accessed Sep. 15, 2022).
[57] Engie. Historical data reports. Online, available at: https://www.engieresources.com/historical-data#reports_anchor, (accessed on Sep. 15, 2022).
[58] Gurobi Optimization L.L.C. Gurobi Optimizer Reference Manual, 2021. Online, available at: https://www.gurobi.com, (accessed Sep. 15, 2022).

[59] T. Singh. Smart home dataset with weather information. Online, available at: https://www.kaggle.com/datasets/taranvee/smart-home-dataset-with-weather-information, (accessed Sep. 15, 2022).

[60] M. Tostado-Véliz, S. Kamel, F. Aymen, F. Jurado. A novel hybrid lexicographic-IGDT methodology for robust multi-objective solution of home energy management systems. *Energy* 2022; 253: 124146. https://doi.org/10.1016/j.energy.2022.124146.

[61] C. Gregory, K. Darby-Downam, G. Mitra. Robust optimization and portfolio selection: The cost of robustness. *European Journal of Operational Research* 2011; 212(2): 417-28. https://doi.org/10.1016/j.ejor.2011.02.015.

[62] F. Wi, Z.X. Jing, P.Z. Wu, Q.H. Wu. A Stackelberg game approach for multiple energies trading in integrated energy systems. *Applied Energy* 2017; 200: 315-29. https://doi.org/10.1016/j.apenergy.2017.05.001.